Precambrian Research 185 (2011) 1–17

Contents lists available at ScienceDirect

Precambrian Research

journal homepage: www.elsevier.com/locate/precamres

Stratigraphic and tectonic implications of field and isotopic constraints on depositional ages of Proterozoic Lesser Himalayan rocks in central Nepal

Aaron J. Martin[a,*], Katherine D. Burgy[a], Alan J. Kaufman[b], George E. Gehrels[c]

[a] Department of Geology, University of Maryland, College Park, MD 20742, USA
[b] Department of Geology and the Earth System Science Interdisciplinary Center, University of Maryland, College Park, MD 20742, USA
[c] Department of Geosciences, University of Arizona, Tucson, AZ 85721, USA

ARTICLE INFO

Article history:
Received 13 December 2009
Received in revised form 28 October 2010
Accepted 18 November 2010
Available online 26 November 2010

Keywords:
Detrital zircon
Calcium carbonate
Lesser Himalayan rocks
Himalaya
Uranium–lead isotopes
Carbon isotopes

ABSTRACT

In the Himalaya of central Nepal, uncertainty in the absolute depositional ages and the relative stratigraphic positions of several formations in the Proterozoic part of the Lesser Himalayan series has hindered structural mapping, east-west correlation of units and structures, and interpretations of basin architecture during both the Proterozoic and Paleozoic. At the stratigraphic base of the Lesser Himalayan series in central Nepal, 441 new U/Pb isotopic ages of detrital zircons from the previously defined type Kuncha, Kushma, and Fagfog formations constrain the maximum possible depositional ages for these clastic units to be c. 1900, 1770, and 1810 Ma, respectively. 182 detrital zircon U/Pb isotopic ages confirm the identity of another sample of the Fagfog Formation, and field relations indicate that this unit rests depositionally on the Kushma Formation with no obvious unconformity or lithologic difference. This interpretation, combined with the recognition that the term "Kushma Formation" historically has been applied incongruously to apparently different units in different parts of Nepal, leads us to recommend abandoning the term "Kushma Formation" and replacing it with "lower Fagfog Formation." The overlying part of the Fagfog then becomes the "upper Fagfog Formation." Because the 1770 Ma constraint on the maximum depositional age comes from the lower part of the unit, the entire Fagfog Formation must have been deposited after 1770 Ma. The depositional ages of both the lower and upper parts of the Fagfog must be younger than the Kuncha Formation because it was intruded by a granite at 1878 ± 22 Ma (2-sigma). Thus an unconformity lasting at least 86 M.y. probably separates the Kuncha Formation (deposited between 1900 and 1856 Ma, considering uncertainties) and the Fagfog Formation (deposited after 1770 Ma). The lower Fagfog Formation is present in the Kali Gandaki region but apparently pinches out to the east because it is not present structurally beneath the Kathmandu nappe.

Suggestions about the depositional age of the carbonate-dominated Malekhu Formation at the top of the Proterozoic part of the Lesser Himalayan series have ranged from Mesoproterozoic to late Paleozoic. These age estimates largely stem from correlation with parts of the Krol succession some 500 km to the west in northwest India, and changing interpretations of the depositional age of the Krol rocks. 104 new measurements of carbon isotope abundances in carbonate from a 300 m measured section through type exposures of the Malekhu Formation reveal a narrow range of $\delta^{13}C$ values between −1.7 and +0.2‰ (VPDB) and a mean of −0.9 ± 0.4‰ (1 standard deviation). These values are inconsistent with correlation with the Krol succession, which preserves large amplitude positive and negative excursions in $\delta^{13}C$ values. Comparison with known marine carbonate $\delta^{13}C$ values through time suggests deposition of the Malekhu Formation prior to c. 1300 Ma. Upper and lower bounds for deposition of the Proterozoic part of the Lesser Himalayan series thus are c. 1300 and c. 1900 Ma, though actual deposition likely occurred during only a portion of this interval. Further, a profound unconformity representing at least 900 M.y. separates the Malekhu Formation from the depositionally overlying Carboniferous-Permian Sisne Formation. No upper Mesoproterozoic, Neoproterozoic, or lower Paleozoic rocks have been found in the Lesser Himalayan series in central Nepal. The carbon isotope stratigraphy of the Malekhu Formation in central Nepal matches that of the Buxa Formation exposed in the Ranjit window of Sikkim to the east, but does not match the chemostratigraphy of rocks correlated with the Buxa Formation in eastern Bhutan and Arunachal Pradesh, northeast India.

* Corresponding author. Tel.: +1 301 405 5352; fax: +1 301 405 3597.
E-mail address: martinaj@geol.umd.edu (A.J. Martin).

0301-9268/$ – see front matter © 2010 Elsevier B.V. All rights reserved.
doi:10.1016/j.precamres.2010.11.003

1. Introduction

Elucidating along-strike geologic relationships is an important key to understanding the tectonics of a fold-and-thrust belt, including the important advance of incorporating a three-dimensional perspective of the orogen into conceptual and computational models. Correlations of stratigraphy and structures along strike are interrelated and particularly important tasks in this process. Differences in along-strike stratigraphy have a multitude of implications. Most obviously, stratigraphic contrasts point to differential basin development at the time of deposition. When these rocks become stacked in thrust sheets, disparities in stratigraphic thickness may result in variable orogenic wedge thickness along strike in the thrust belt, even if the geometries and kinematics of structures are similar. Unequal thrust sheet thicknesses produce different metamorphic conditions, and different wedge thicknesses may generate variable crustal thicknesses and thus variable surface elevations. Further, different vertical distributions of rock types result in dissimilar strength profiles through the upper crust, which in turn can produce distinct structural styles along strike, even given the same convergence, shortening, and stresses.

Constraining along-strike stratigraphic relations requires detailed knowledge of the stratigraphy at multiple sites. This paper focuses on the depositional ages and stratigraphy of the Proterozoic part of the Lesser Himalayan series in central Nepal (Fig. 1). The depositional ages of the formations that comprise the Proterozoic part of the Lesser Himalayan series have been poorly constrained largely due to (1) the absence of fossils, except for stromatolites near the stratigraphic top, and (2) the scarcity of igneous rocks suitable for radiometric dating, except for c. 1780–1880 Ma meta-granites that intruded near the stratigraphic base (DeCelles et al., 2000; Chambers et al., 2008; Celerier et al., 2009; Kohn et al., 2010). Although U/Pb isotopic ages of detrital zircons from some of these Lesser Himalayan rocks in Nepal have been published (Parrish and Hodges, 1996; DeCelles et al., 2000; Martin et al., 2005), uncertainties about absolute and relative depositional ages of some of the units remain due to two issues. First, for many samples, an insufficient number of detrital zircons were dated to produce age peaks composed of multiple dates. Multi-date peaks increase confidence in interpretations of the depositional age significance of the analyses (Dickinson and Gehrels, 2009). Second, identification of particular formations was not the focus of these studies and some samples were identified as coming from lower Lesser Himalayan rocks in general rather than from specific formations. Nevertheless, the age constraints provided by these studies, combined with the recognition that the rocks do not contain fossils except for stromatolites, led to the conclusions that at least the lower formations were deposited in mid-late Paleoproterozoic time and that the remainder probably were deposited in the Proterozoic as well (Stocklin, 1980; Upreti, 1996, 1999; Parrish and Hodges, 1996; DeCelles et al., 2000; Dhital et al., 2002; Robinson et al., 2006; Kohn et al., 2010).

One unit near the base of the Lesser Himalayan series in Nepal, the Kushma Formation, has been interpreted inconsistently by different workers over the past three decades. Many stratigraphers did not include the Kushma Formation; these workers placed the Kuncha Formation or an equivalent unit at the base of the Lesser Himalayan series in central Nepal (Fig. 1; Stocklin, 1980; Sakai, 1983, 1985; Upreti, 1996, 1999; Dhital et al., 2002). In contrast, the geologic map of west-central Nepal by Tater et al. (1983) introduced the quartzite-rich Kushma Formation in the lower part of the Lesser Himalayan series, but not at its base. The type locality of the Kushma Formation is in the hills north of the town of Kushma, Parbat district, near the confluence of the Kali Gandaki and Modi rivers, and is shown on this 1983 map. Some subsequent maps by this group incongruously applied the Kushma Formation name not to the quartzite-rich unit above the base of the Lesser Himalayan series as at the type locality (stratigraphically above the Ranimata Formation), but to an apparently different quartzite-rich unit at the stratigraphic base of the succession (below the Ranimata Formation; Shrestha et al., 1984, 1987a,b,c). DeCelles et al. (1998) followed these Department of Mines and Geology maps for western Nepal and used the Kushma Formation name for the stratigraphically basal, quartzite-rich unit in western Nepal. Subsequent papers by DeCelles and colleagues continued this practice (e.g., DeCelles et al., 2001; Pearson and DeCelles, 2005; Robinson et al., 2006; Robinson, 2008). Lost over the decades of stratigraphic and structural work, however, is the recognition that the term “Kushma Formation” inappropriately has been applied to two apparently different quartzite-rich formations in different parts of Nepal. Reconciliation of these different stratigraphic schemes is critically important both for structural interpretations and for east-west correlations. In this paper we constrain the maximum possible depositional ages of the oldest formations of the Lesser Himalayan series in central Nepal (Kuncha, Kushma, and Fagfog formations) using new U/Pb isotopic dates of detrital zircons from samples taken at their type localities. Using these data in combination with field evidence and the crystallization ages of granites that intruded the Kuncha Formation, we clarify the stratigraphy of the lowermost part of the Lesser Himalayan series and show the importance of this clarification for stratigraphic correlations and geologic mapping.

Age relationships near the stratigraphic top of the Proterozoic part of the Lesser Himalayan series have been as unclear as those at the stratigraphic base. At this stratigraphic position, the Sisne Formation, a Gondwanan clastic unit probably deposited in the Carboniferous to Permian, unconformably overlies the Malekhu Formation, a stromatolite-bearing, carbonate-rich unit of presumed late Proterozoic depositional age (Fig. 1; Upreti et al., 1980; Sakai, 1983; Upreti, 1996, 1999). However, the depositional age of the Malekhu is poorly known, with published suggestions ranging over one billion years from the Mesoproterozoic to the late Paleozoic (Stocklin, 1980; Sakai, 1983, 1985; Upreti, 1996, 1999; DeCelles et al., 2001; Pearson and DeCelles, 2005). The suggestion of a late Neoproterozoic depositional age largely is based on possible correlation of the Malekhu and related rocks in Nepal with parts of the terminal Neoproterozoic Krol succession 500 km to the west in northwest India (Hagen, 1969; Fuchs and Frank, 1970; Sharma et al., 1984; Dhital et al., 2002), as well as on identification of stromatolite forms (Upreti et al., 1980). Better constraints on the depositional age of the Malekhu Formation, as well as a comparison of carbon isotope stratigraphy, are important for confirming or refuting the correlation with the Krol succession to the west.

Tighter bounds on the depositional age of the Malekhu are also important for reconstructing the Neoproterozoic to early Paleozoic tectonic and depositional history of the Lesser Himalayan series and its relationship to the structurally overlying Greater Himalayan and Tethyan Himalayan successions. The apparent absence of lower Paleozoic strata across the unconformity between the Proterozoic Malekhu and Carboniferous-Permian Sisne formations in Nepal is an important feature of many such reconstructions (Saxena, 1971; Searle, 1986; Aharon et al., 1987; Brookfield, 1993; Upreti and Le Fort, 1999; Corfield and Searle, 2000; DeCelles et al., 2000). Indeed, the interpretation that Cambrian rocks are present in the Lesser Himalayan series in northwest India forms the basis of an argument supporting one class of these models (Myrow et al., 2003). Better constraints on the depositional age of the Malekhu Formation can help inform this debate. In

Depositional Age	Formations this study	Formations from Upreti, 1996		Formations from Tater et al. (1983)	Other Tater et al. (1983) formations
Miocene	Dumri	Dumri	Tansen Unit	Suntar	
Eocene	Bhainskati	Bhainskati		Swat	
Carboniferous-Paleocene	Gondwanan Unit	Gondwanas		(not present)	
	(not present)	Robang	Nawakot Unit	(not present)	
Meso-proterozoic (?)	Malekhu	Malekhu		Lakharpata	
	Benighat	Benighat			
	Dhading	Dhading			
	Syangja	Nourpul		Syangja	←Sangram
	Galyang	Dandagaon		Galyang	←Ghan Pokhara
Paleo-proterozoic	upper Fagfog	Fagfog		Naudanda	←Seti (Kuncha equivalent)
	lo. Fagfog			Kushma	
	Kuncha (including meta-diorite and meta-granite)	Kuncha (including meta-diorite and Ulleri meta-granite)		Ranimata (to west) and Ulleri	

Fig. 1. Our generalized stratigraphic column through Lesser Himalayan rocks in central Nepal compared to the columns by Upreti (1996) and Tater et al. (1983). The rightmost column lists units named by Tater et al. (1983) that either are abandoned or included in other formations in the other columns. The lower portion of the Fagfog Formation appears to pinch out to the east. The Gondwanan Unit consists of several formations; from base to top these are the Sisne, Taltung, and Amile formations.

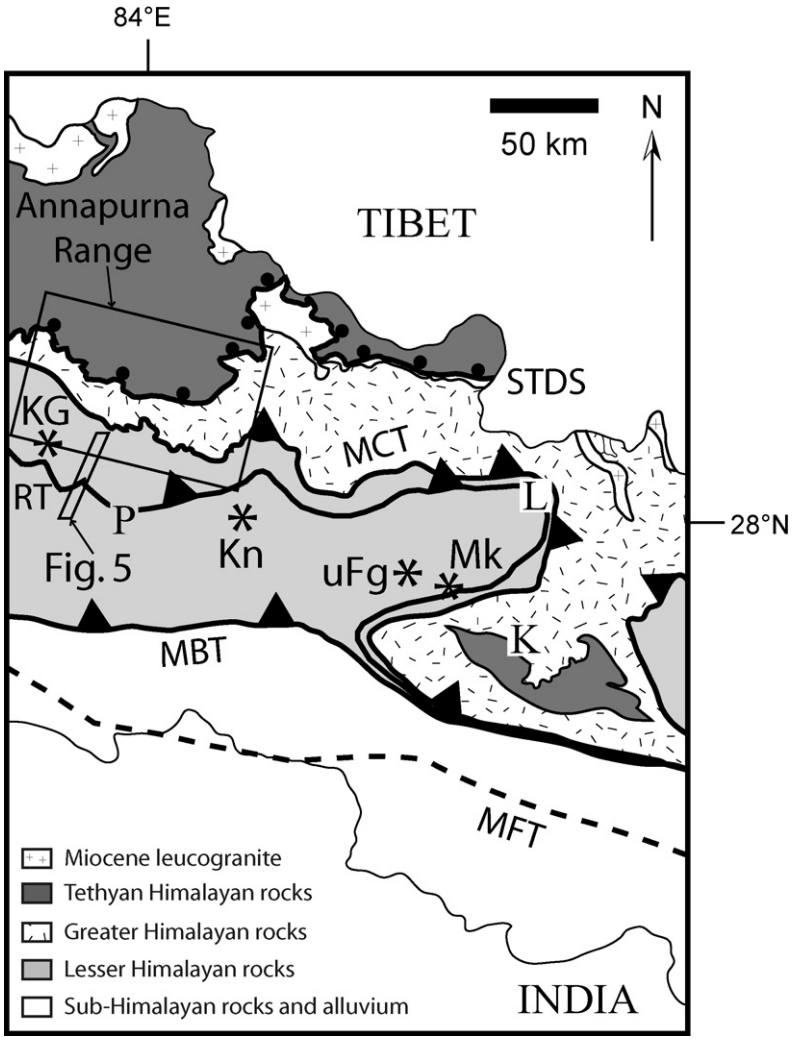

Fig. 2. Generalized geologic map of central Nepal modified from Amatya and Jnawali (1994). Stars mark the location of the samples of the type upper Fagfog (uFg), Kuncha (Kn), and Malekhu (Mk) formations, and of sample KG-1 (KG). Other abbreviations: MBT – Main Boundary thrust, MCT – Main Central thrust, MFT – Main Frontal thrust, RT – Ramgarh thrust, STDS – South Tibetan Detachment System. Areas: K – Kathmandu, L – Langtang, P – Pokhara. The box outlining the location of the Annapurna Range is approximate. The line for the MFT is dashed because its location is approximate.

this paper, we place a limit on the minimum depositional age of the Malekhu Formation using carbon isotopes from carbonate collected in the framework of a measured section through the type locality of the Malekhu Formation in central Nepal (Fig. 2).

2. Geologic setting

The Lesser Himalayan series is bounded by two major thrusts (Fig. 2). At the structural top of the series, the Main Central thrust placed Greater Himalayan pelitic, psammitic, and meta-carbonate rocks on Lesser Himalayan metasedimentary rocks via ductile shearing starting before c. 23 Ma and ending about 15 Ma (Hodges et al., 1996; Kohn et al., 2004). At the structural base, the Main Boundary thrust placed Lesser Himalayan metasedimentary rocks over Neogene sub-Himalayan foreland basin clastic rocks at c. 5 Ma (DeCelles et al., 1998). Numerous other thrusts and normal faults cut Lesser Himalayan rocks, most importantly the Ramgarh thrust (DeCelles et al., 1998; Pearson, 2002; Pearson and DeCelles, 2005; Robinson et al., 2006; Robinson, 2008). Depositional basement for the Lesser Himalayan series does not outcrop in Nepal and generally is thought not to be exposed anywhere in the Himalaya, though there are exceptions to this interpretation (e.g., Valdiya, 1995; Miller et al., 2000; Celerier et al., 2009).

The Lesser Himalayan series primarily consists of sedimentary rocks, most of which were metamorphosed to sub-greenschist through lower amphibolite facies, depending on location (e.g., Beyssac et al., 2004; Martin et al., 2010a). However, the basal formation was intruded by several different granite bodies as well as by unnamed dioritic rocks, both of which are also part of the Lesser Himalayan series (Fig. 1). The lower part of the Lesser Himalayan series, called the Nawakot Unit in central Nepal, mostly consists of metamorphosed Paleo- and Mesoproterozoic shale, muddy sandstone, and sandstone (Stocklin, 1980; Sakai, 1983, 1985; Upreti, 1996, 1999; Robinson et al., 2006). Two thick Proterozoic metacarbonate-rich formations occur near the stratigraphic top of the Nawakot Unit, and in this report we study the uppermost, the Malekhu Formation. The upper part of the Lesser Himalayan series, called the Tansen Unit in Nepal, is composed of clastic Carboniferous to Paleocene Gondwanan deposits and Eocene to lower Miocene Himalayan foreland basin strata (Stocklin, 1980; Sakai, 1983, 1985; Upreti, 1996, 1999; DeCelles et al., 2004).

In this paper we focus on formations near the stratigraphic base and top of the Proterozoic Nawakot Unit (Fig. 1). In the following paragraphs we describe the lithology of each Nawakot Unit formation in central Nepal, beginning with the top of the succession (see also Stocklin, 1980; Sakai, 1983, 1985; Upreti, 1996, 1999; Dhital et al., 2002; Kohn et al., 2010). All of these rocks have been metamorphosed to facies ranging from sub-greenschist to lower amphibolite, depending on location. Because this paper focuses on stratigraphy rather than metamorphism, we describe the rocks in terms of their sedimentary protoliths. Discussion of the metamorphism of these and Greater Himalayan rocks can be found in Martin et al. (2007, 2010a) and references therein.

Malekhu Formation protoliths: Dominantly light to medium gray limestone and dolostone (Fig. 3). Stromatolites and especially planar-laminated algal structures are common in low-grade exposures, though well-formed, domal stromatolites typically are less abundant than in the older, carbonate-rich Dhading Formation. At the type section, the grain size is mostly fine sparite, and the dolostones typically have slightly larger grains than the limestones (Fig. 3A and C). Many samples from the type section also contain coarser-grained portions. Grain sizes are much larger at locations where the Malekhu experienced higher grade metamorphism. The Malekhu also contains interbedded light to dark gray calcareous shale up to 40 m thick (Fig. 3B). At the type section, the mean length

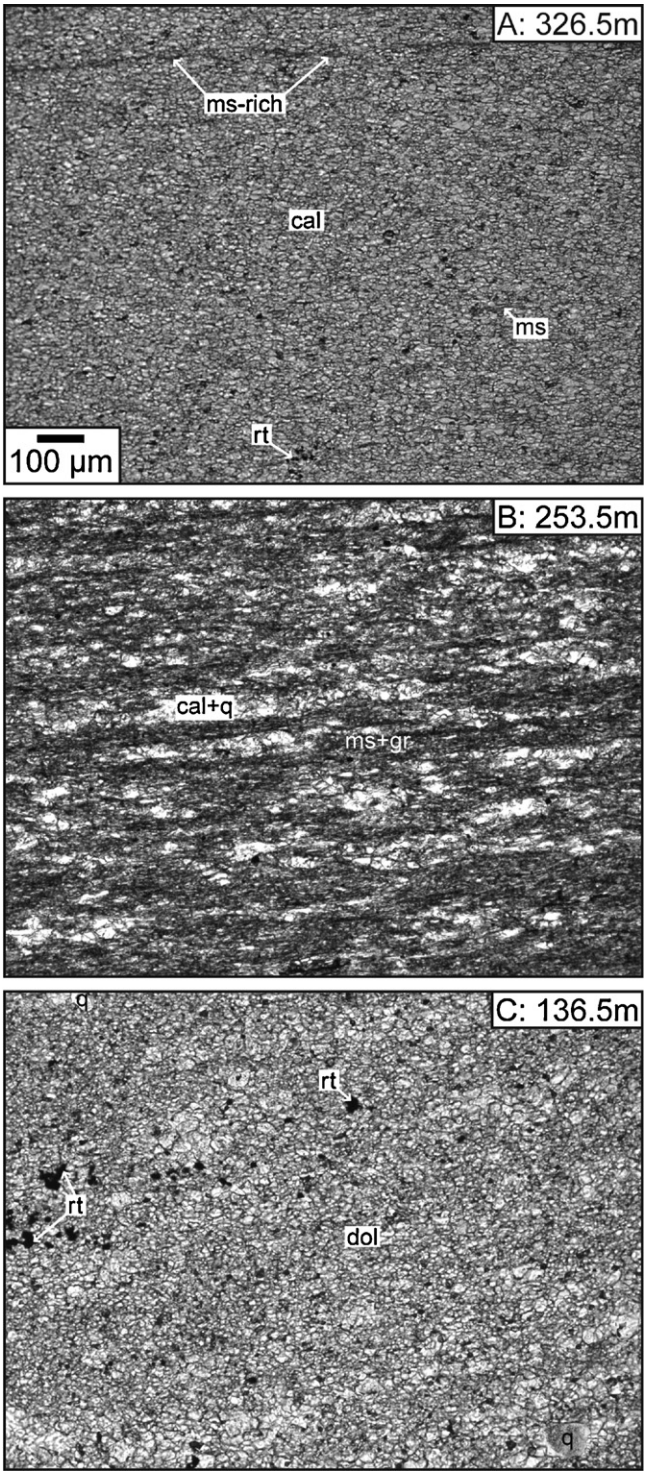

Fig. 3. Photomicrographs of thin sections through meta-carbonates from the measured section through the type locality of the Malekhu Formation. (A) Limestone collected at 326.5 m above the base of the measured section showing muscovite-rich lamination. (B) Calcareous shale from 253.5 m. (C) Dolostone from 136.5 m. The scale is the same for all images. Plane-polarized, transmitted light. Abbreviations: cal – calcite, dol – dolomite, gr – graphite, ms – muscovite, q – quartz, rt – rutile.

in thin section of the long axes of the carbonate grains in the calcareous shales is about 20–30 μm, but increases near the Ramgarh thrust to about 170 μm. The Carboniferous-Permian Sisne Formation depositionally overlies the Malekhu, but is not widely exposed except in parts of central and western Nepal (Sakai, 1983; Upreti, 1996).

Benighat Formation protolith: Black shale. Thin carbonate beds near the top and base are included in the Benighat by some workers, but in the Malekhu or Dhading Formation by others.

Dhading Formation protoliths: Dominantly light to medium gray limestone and dolostone. Stromatolites and planar-laminated algal structures are abundant in low-grade outcrops. The Dhading also contains interbedded calcareous shale.

Syangja Formation protoliths: Interbedded sandstone, shale, and limestone. Sandstone and shale commonly is distinctively pink, lavender or purple, although sandstone can be white to tan and shale can be gray, green, maroon, or brown. Limestone is white to gray or brown. Sandstone typically is fine- to coarse-grained arenite composed of about 70% quartz and feldspar and 30% lithics. Cross-stratification, ripple casts, and mud cracks are present in many outcrops. The Syangja is called the Nourpul Formation by some workers (Upreti, 1996).

Galyang Formation protolith: Medium gray shale. Shale color varies from light gray to black. The Galyang is called the Dandagaon Formation by some workers (Upreti, 1996).

Upper Fagfog Formation protoliths: Dominantly very fine- to medium-grained, white to yellow quartz arenite with a light green tint in places (Fig. 4A). Sand grains are 95–99% quartz. There are fewer sedimentary lithic clasts in the upper part compared to the lower part of the Fagfog Formation. Trough cross-beds occasionally are present and ripple casts are very common in low-grade, moderately or minimally deformed outcrops. The upper Fagfog also contains minor interbedded shale, which commonly is green after metamorphism. This shale generally is less than 5 m thick, but some map-scale bodies exist (Fig. 5). The upper Fagfog also contains minor interbedded muddy sandstone with 75% fine sand. Typical outcrops have rippled quartz arenite beds 10–60 cm thick separated by sandy shale beds that are 1–10 cm thick. It is difficult to distinguish lower from upper Fagfog in many outcrops, including at the top of the type lower Fagfog. The upper Fagfog is called the Naudanda Formation by some workers (Dhital et al., 2002).

Lower Fagfog Formation protoliths: Dominantly medium- to coarse-grained, white to yellow quartz arenite with a light green tint in places (Fig. 4B). Quartz granule conglomerate is also present. Sand and granule grains are 95–99% quartz. Some grains are fragments of fine-grained sandstone (Fig. 4B). This protolith sandstone had more mud and more non-quartz grains than the quartz arenites of the lower Fagfog Formation, demonstrating that the lower Fagfog sediments were derived in part from weathering and erosion of previously existing, less-mature sandstone. Trough cross-beds and ripple casts are observed infrequently in low-grade, moderately or minimally deformed exposures. The lower Fagfog also contains rare interbedded shale, usually green after metamorphism and less than 5 m thick. Typical outcrops have one-half to 2 m thick sandstone separated by 1–10 cm thick sandy shale beds. The lower Fagfog was called the Kushma Formation by Tater et al. (1983).

At many outcrops of the Fagfog Formation, including at the top of the type lower Fagfog exposures, it is clear that the rocks belong to the Fagfog but difficult to assign them to either the upper or lower part of the formation using field-based criteria. Possible distinguishing characteristics include a greater abundance of ripple casts in sandstone of the upper Fagfog Formation and coarser grain sizes in lower Fagfog sandstone. Neither feature is diagnostic, however. Some outcrops of lower Fagfog Formation sandstone contain ripple casts, whereas some exposures of upper Fagfog sandstone do not, especially outcrops of moderately or intensely deformed or metamorphosed beds. The two units have an overlapping range in grain sizes, and grain sizes can be altered during deformation and metamorphism. Further, it appears that at the type locality along the Modi Khola, lower Fagfog Formation sandstones become finer-grained stratigraphically upward, making the contact with the upper Fagfog difficult to recognize in the field (Fig. 5). There is not an obvious unconformity between the lower and upper Fagfog formations at this location that would facilitate such recognition.

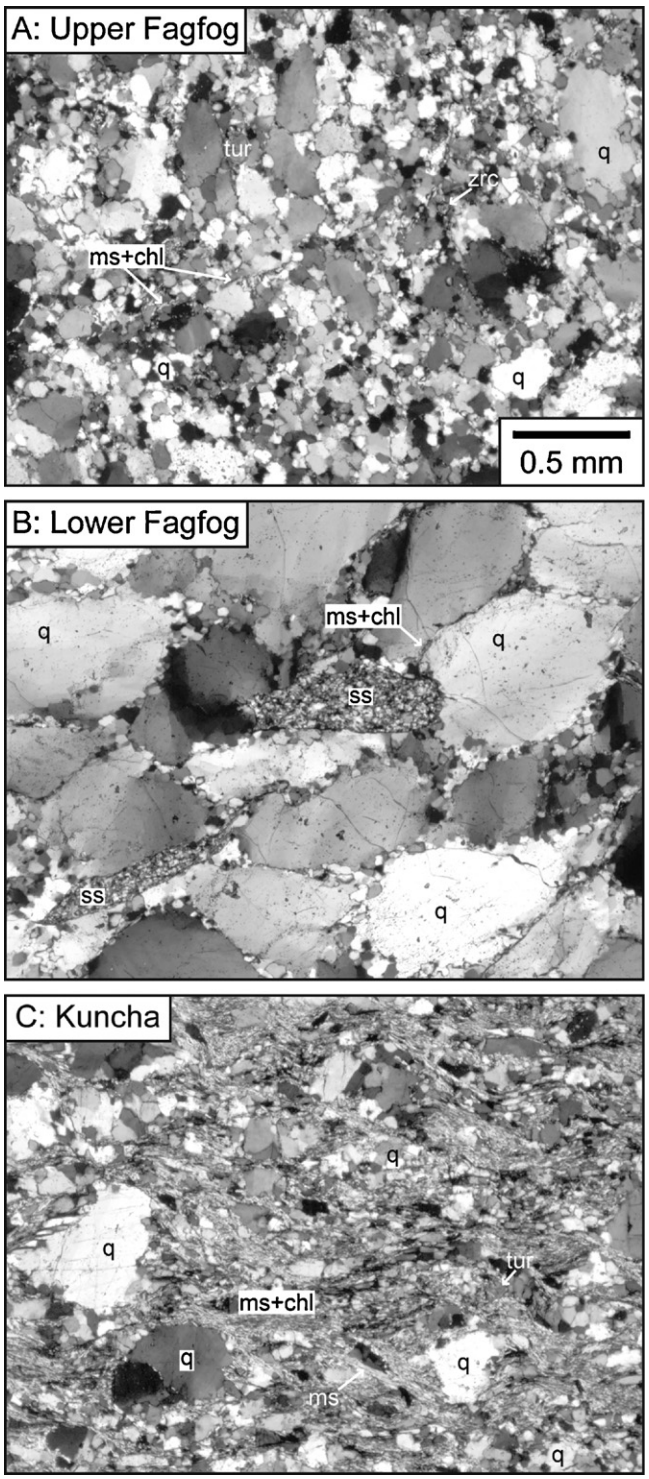

Fig. 4. Photomicrographs of thin sections through meta-sandstones from the type localities of the Kuncha, lower Fagfog, and upper Fagfog formations. Tourmaline, muscovite, and chlorite in all three samples are of metamorphic origin, not detrital. The scale is the same for all images. Cross-polarized, transmitted light. Abbreviations: chl – chlorite, ms – muscovite, q – quartz, ss – sandstone lithic fragment, tur – tourmaline.

Kuncha Formation protoliths: Mostly muddy sandstone, 60–80% sand grains (Fig. 4C). Sandy mudstone, 20–40% sand, is also common. The Kuncha also contains minor shale (less than 10% sand, often green after metamorphism) and arenite (more than 90%

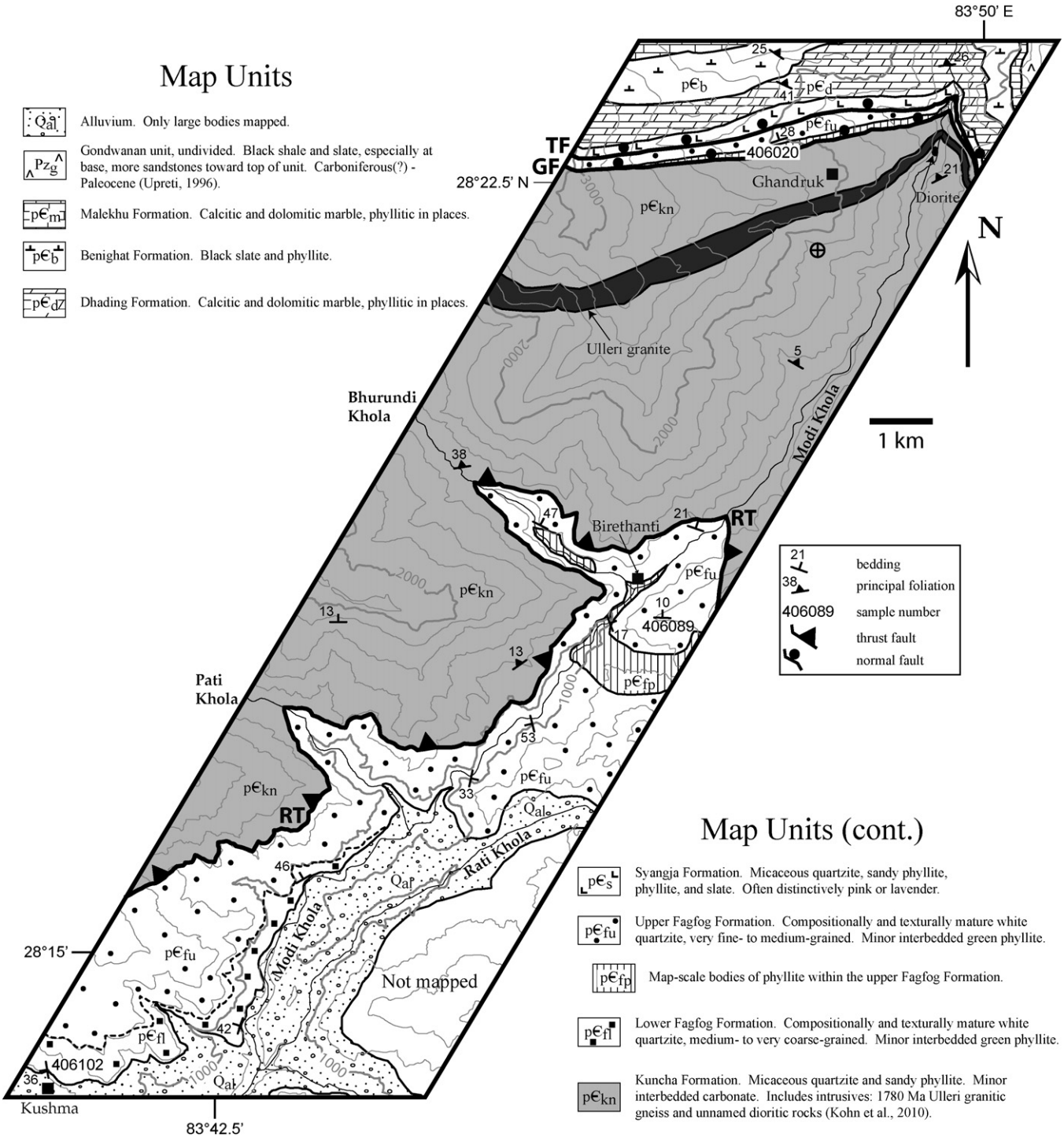

Fig. 5. Geologic map of part of the Modi Khola valley, central Nepal. Strike-and-dip symbols show the locations of numbered samples. RF – Romi fault, RT – Ramgarh thrust, TF – Tobro fault. The contact between the lower and upper parts of the Fagfog Formation is dashed because the location is approximate. The square that marks the town of Kushma is at the northwestern edge of the town. Contour interval: 200 m.

sand). Sand grain size is typically medium to coarse, and rocks with more mud content usually have finer-grained sand. Sand grains are somewhat compositionally immature, with 5–40% plagioclase feldspar and lithics. Sedimentary structures are extremely uncommon. Typical outcrops have interbedded muddy sandstone (dominant) and sandy mudstone (subordinate) with individual beds 10–60 cm thick, and much less abundant shale, 1–10 cm thick. The Kuncha Formation was intruded by several different granites, including a c. 1880 Ma meta-granite in the Langtang region and the c. 1780 Ma Ulleri meta-granite in the Annapurna Range (Celerier et al., 2009; Kohn et al., 2010), and by unnamed dioritic rocks. The depositional basement for the Kuncha Formation is not exposed.

Kohn et al. (2010) suggest that parts of the Kuncha Formation consist of metamorphosed felsic tuffs and volcaniclastic rocks. Using visual criteria, generally it is difficult to discriminate between a muddy, poorly sorted sandstone and a felsic tuff or volcaniclastic rock after polyphase metamorphism and deformation. However, at the type locality, we did not observe any of the volcanic fea-

tures illustrated by Kohn et al. The muddy sandstone from which we acquired the Kuncha type sample is interbedded with shale and neither rock type appears tuffaceous or volcaniclastic. Therefore we label our zircons from the type sample as detrital, rather than magmatic.

The crystallization age of the Ulleri granite has been difficult to establish accurately. We attempted to date crystallization of the Ulleri granite using zircons extracted from a sample collected at the type locality in central Nepal, but found that accurate dating is hampered by ubiquitous inherited cores and narrow rims no wider than 10 μm. Celerier et al. (2009) experienced similar difficulties in trying to date crystallization of the Ulleri in central Nepal, but tentatively suggested zircon crystallization at c. 1880 and 1800 Ma based on U/Pb isotopic dates near these times. Kohn et al. (2010) interpreted c. 1880 Ma ages from a type sample to be inherited cores and took an intercept of variably discordant to concordant rim analyses at 1780 ± 29 Ma (2 standard deviations, s.d.) to be the crystallization age of the granite. This date overlaps within uncertainties with the 1800 Ma date by Celerier et al. (2009). Accordingly, we use 1780 ± 29 Ma as the crystallization age of the type Ulleri granite in the Annapurna Range. Kohn et al. (2010) dated crystallization of the granite that intrudes the Kuncha Formation in the Langtang region as 1878 ± 22 Ma (2 s.d.), nearly identical to the crystallization age of a meta-tuff interbedded with the Kuncha Formation there. Although the meta-granite in the Langtang region previously was called "Ulleri" based in part on petrologic similarity to the type Ulleri meta-granite, the crystallization ages of the two granites are separated by at least 47 M.y. including uncertainties, so we do not refer to the intrusion in the Langtang region with the name "Ulleri." DeCelles et al. (2000) dated crystallization of a meta-granite in western Nepal at c. 1831 Ma. Kohn et al. (2010) recalculated this age to be 1840 ± 30 Ma. Because the crystallization age of this granite is older than that of the type Ulleri, we likewise do not refer to it with the name "Ulleri". The uncertainties listed for the Kohn et al. ages include measurement uncertainties added quadratically to an additional 1% systematic uncertainty (2 s.d.).

3. Methods

3.1. Detrital zircon U/Pb isotopic dating

Martin collected approximately one-kg samples for detrital zircon dating from the type localities of the Kuncha, lower Fagfog, and upper Fagfog formations and from two Lesser Himalayan quartzites exposed in the Modi Khola valley that we suspected to belong to either the lower or upper Fagfog Formation (Fig. 2; latitudes and longitudes given in Table S1). Gehrels collected an additional sample (KG-1) from an outcrop of suspected Fagfog Formation quartzite in the Kali Gandaki valley north of the town of Kushma, approximately two km south of the town of Tatopani. We label these non-type locality samples as having unknown stratigraphic affinity throughout this article because our field observations do not allow us to discriminate confidently between the lower or upper Fagfog Formation for the sampled outcrops. We separated zircons from each sample using standard techniques including hand crushing and disaggregation, removal of silt and clay by hand panning in water, removal of magnetic grains using a Frantz magnetic barrier separator, and density separation using methylene iodide. We hand-picked approximately 250 randomly chosen zircons from each sample, with no regard for color, size, or shape (120 grains for sample KG-1). Along with about five shards of the Sri Lanka zircon standard (564 ± 3 Ma; Gehrels et al., 2008), we placed the picked zircons in individual mounts, which we then filled with epoxy. We sanded approximately halfway into the mounted zircons by hand and then acquired backscattered electron and cathodoluminescence images of the zircons using the JEOL JXA-8900R electron probe microanalyzer at the University of Maryland (for sample KG-1, imaging took place at the University of Arizona). We removed the carbon coat required for electron beam analysis prior to mass spectrometry by gentle hand polishing and removed common lead on the mount surface by soaking the mounts for five min in dilute nitric acid.

For all samples except KG-1, we dated the cores of about 200 detrital zircons from each sample by ablating individual cores using a laser with a beam diameter of 25 or 30 μm followed by isotopic analysis using the GV Instruments Isoprobe multi-collector inductively coupled plasma mass spectrometer housed in the Arizona LaserChron Center at the University of Arizona. For KG-1 we followed this procedure, but dated the cores of 100 detrital grains. We used the backscattered electron and cathodoluminescence images to guide our placement of the laser spot in each zircon, taking care to avoid: (1) ablating multiple cathodoluminescence zones due to overlap by the laser spot, (2) inclusions, and (3) cracks. Details of the analytical protocols are given in Gehrels et al. (2008).

We followed the data reduction procedures outlined by Gehrels et al. (2008), removing from further consideration analyses with: (1) high ^{204}Pb, (2) low ^{206}Pb/^{204}Pb ratio, (3) greater than 5% error on the ^{206}Pb/^{207}Pb date, (4) greater than 10% error on the ^{206}Pb/^{238}U date, (5) greater than 25% normal discordance or 5% reverse discordance, (6) high U concentration, or (7) high U/Th ratio. Because all remaining analyses for the samples discussed in this paper yielded only ^{206}Pb/^{207}Pb and ^{206}Pb/^{238}U dates much older than 1200 Ma and ^{206}Pb/^{207}Pb dates usually are more accurate for grains older than about 1200 Ma, we used each ^{206}Pb/^{207}Pb date as the crystallization age of the corresponding zircon. Although we applied the filters listed in this paragraph mostly to reject grains compromised by lead loss and/or metamorphic zircon growth, it is not possible to be certain that any individual analysis has not been so compromised, particularly for the youngest ages in a population. Accordingly, we attach maximum possible depositional age significance only to clusters of three or more ages with measurement errors that overlap at the 1-sigma level (cf. Dickinson and Gehrels, 2009). To obtain a number for the maximum depositional age, for each analysis we first quadratically added the random measurement error to the non-random systematic uncertainty, which is approximately 1% (2 s.d.) for the ^{206}Pb/^{207}Pb ages from all the samples. We then added the weighted mean of the three youngest overlapping ages as defined above to the 2-sigma uncertainty on that mean and rounded up to the nearest 10 M.y. increment. Such rounding avoids the spurious precision of a significant figure in the ones place. For example, if the three youngest overlapping analyses yield a weighted mean of 1801 ± 23 Ma (2 s.d.), we use 1830 Ma as the maximum depositional age – at the 95% confidence level we can state that the rock was not deposited before 1830 Ma. This technique has the advantage that it is insensitive to the number of grains used to estimate the maximum depositional age, but the disadvantage that it calculates a mean for multiple grains that truly might have crystallized at different times. The mean squared weighted deviates (MSWD) value can be used to help assess the validity of this calculation.

We assigned the outcrops of suspected Fagfog Formation (which we label "unknowns" throughout this article) to the lower or upper part of the formation by comparing the U/Pb isotopic ages of the detrital zircons from the samples of these units to the detrital zircon age signatures from the samples from the type localities. These comparisons use all the ages in the detrital zircon suites, not only the youngest grains. This stratigraphic correlation method relies on the assumption that the detrital zircon age signature changes only minimally within an individual formation (or part of a formation in the case of the lower and upper Fagfog). This assumption can be strengthened by dating multiple samples from the type localities

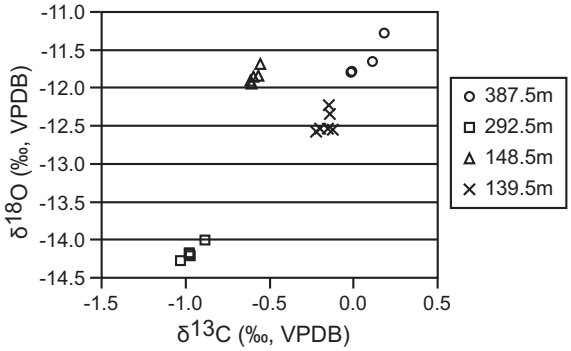

Fig. 6. Plot of $\delta^{18}O$ versus $\delta^{13}C$ values for multiple drill sites in the same polished section from four different samples. Intra-sample variability is generally small, so isotopic values of powder from any single drill site generally are representative of the values for the entire carbonate texture that was sampled. Measurement uncertainty is the same as or smaller than the size of the symbols.

of the formations, but it can never be shown to be correct because it is always possible that the next dated sample might yield different ages. We have not found evidence for major changes in detrital zircon age signatures within the Kuncha, lower Fagfog, and upper Fagfog formations in central Nepal.

3.2. Malekhu Formation carbonate C and O isotope measurement

Burgy used a Jacob's staff to measure a section through the Malekhu Formation at its type locality near the town of Malekhu in central Nepal (dirt road along the Trishuli Ganga River north of the town of Galcchi Bazar; base of exposed section at 27.84136°N, 85.02327°E). She collected an approximately 0.25 kg sample for carbonate C and O isotope analysis every three m and at obvious lithologic changes. For isotope analysis we followed the analytical procedures outlined in Kaufman and Knoll (1995). At the University of Maryland, we cut and polished each sample and then selected sites within it for microsampling with a drill. Drilled spots were in visually homogenous, fine-grained parts of the rock far removed from veins, cracks, or weathered surfaces. We acidified 100 μg of the drilled rock with concentrated phosphoric acid (density = 1.89 g/cm^3) under vacuum for 10 min at 90 °C and measured C and O isotopes in the resulting CO_2 gas using the GV Instruments IsoPrime dual inlet gas source mass spectrometer at the University of Maryland. We interspersed analyses of NBS-19 standard during analysis of the Malekhu Formation samples and calculated the isotopic results relative to the Vienna PeeDee Belemnite (VPDB) scale. The mean measurement errors for $\delta^{13}C$ and $\delta^{18}O$ were 0.03‰ and 0.08‰, respectively, and were always less than 0.07‰ and 0.17‰, respectively.

In order to ensure that the C and O isotopic values for the drilled spot in each polished section through the Malekhu Formation carbonates represent the isotopic composition of the entire carbonate texture that was sampled, we measured the C and O isotopic ratios for multiple spots in each of four samples. Fig. 6 shows the results of this test and Table S2 contains the isotopic data. In general, variability in the isotopic ratios is quite limited: most of the measurements from each sample are within analytical uncertainty of each other. However, some analyses from some samples, particularly those from the sample at 387.5 m in the measured section, fall outside measurement error of one another, indicating isotopic heterogeneity of up to a few tenths of one per mil at the scale of a few millimeters in some samples. The magnitude of this heterogeneity is small compared to the variability in C and O isotopic ratios throughout the measured section. Intra-sample $\delta^{13}C$ and $\delta^{18}O$ values vary by no more than 0.2‰ and 0.5‰, respectively.

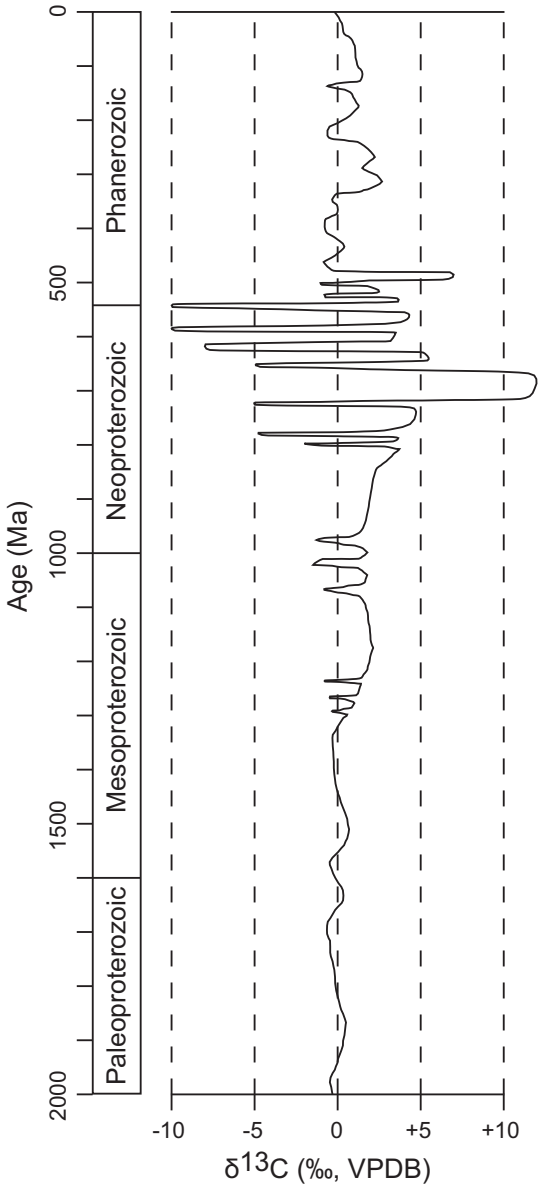

Fig. 7. $\delta^{13}C$ values of marine carbonate during the Phanerozoic and most of the Proterozoic. Note the long period between c. 2000 and 1300 Ma during which $\delta^{13}C$ values were near 0‰. We do not show the period before 2000 Ma because all exposed Lesser Himalayan metasedimentary rocks were deposited after c. 1900 Ma. Modified from Bartley and Kah (2004) using data in Bartley et al. (2001) for the late Meso- to early Neoproterozoic; Kaufman et al. (1997, 2006, 2007), Halverson et al. (2005), Fike et al. (2006), Misi et al. (2007), and McFadden et al. (2008) for the Neoproterozoic; and Kaufman et al. (2009) for the Cambrian.

We obtained a constraint on the minimum depositional age of the Malekhu Formation by comparing trends in the carbonate $\delta^{13}C$ values from the measured section with known marine carbonate $\delta^{13}C$ values throughout the Proterozoic and Paleozoic intervals. Between c. 2000 and 1300 Ma, marine carbonates preserved $\delta^{13}C$ values with remarkably little variability; most values lie within 2‰ of zero (Fig. 7; Buick et al., 1995; Knoll et al., 1995; Frank et al., 1997; Xiao et al., 1997; Kah et al., 1999; Lindsay and Brasier, 2000; Kumar et al., 2002; Bartley and Kah, 2004). In contrast, during the period c. 1300–500 Ma, marine carbonates recorded profound positive and negative excursions in $\delta^{13}C$ values superimposed on a background enriched in ^{13}C (e.g., Kaufman and Knoll, 1995; Kah et al., 1999; Bartley et al., 2001; Kumar et al., 2002; Bartley and Kah, 2004; Halverson et al., 2005; Maloof et al., 2005; Kaufman et al., 2006,

2007, 2009; Tewari and Sial, 2007). Immediately after c. 1300 Ma, values near +3.5‰ dominated (Bartley et al., 2001).

At its type locality, the metamorphic grade of the Malekhu Formation is poorly known. Nearby pelites that, like the Malekhu, are structurally below the Ramgarh thrust do not bear garnet and appear to be in the chlorite zone, which suggests lower greenschist facies metamorphism. Several workers have shown that diagenesis and low-grade regional metamorphism commonly only minimally affect $\delta^{13}C$ values in carbonate, but frequently alter corresponding $\delta^{18}O$ values (Tucker, 1985; Knoll et al., 1986; Fairchild and Spiro, 1987; Burdett et al., 1990; Kaufman et al., 1991; Jacobsen and Kaufman, 1999). The most likely explanation for this difference is that most meteoric and regional metamorphic fluids are dominated by water, which has abundant O, but contain little C relative to the vast amount of C present in the carbonate. However, it is important to note that there are published examples of post-depositional alteration of $\delta^{13}C$ values (e.g., Zempolich et al., 1988; Fairchild et al., 1990; Kaufman et al., 1992). We take the measured C isotopic ratio of the drilled portion of each rock to be near the depositional value and interpret the vertical succession of the values to constrain the depositional age, whereas we infer that the measured O isotopic ratios have been altered away from depositional values by metamorphism and so do not interpret them further.

4. Results

4.1. Detrital zircon U/Pb isotopic dating

Fig. 8 shows histograms and relative probability plots for the U/Pb isotopic ages of the detrital zircons from the six quartzite samples, and Figure S1 shows the corresponding concordia plots. Table S1 contains the isotopic and concentration data as well as the sample locations (shown in Figs. 2 and 5).

Analysis of zircons from the sample of type Kuncha Formation micaceous quartzite (sample number 506078) yielded 135 usable dates, which were bracketed by 27 standard analyses. One standard deviation of the $^{206}Pb^*/^{207}Pb^*$ and $^{206}Pb^*/^{238}U$ ratio for the standard grains was 0.67% and 1.6%, respectively (Pb* refers to radiogenic Pb). By far the largest age peak in this sample is at c. 1900 Ma; there are also a few much smaller older peaks, most prominently at c. 2510 Ma (Fig. 8). There is one young analysis at 1839 ± 24 Ma (grain 30), but we do not attach depositional age significance to it because it does not form a cluster of three or more ages. Grains 63, 60, and 152 yielded ages of 1849 ± 29, 1867 ± 18, and 1868 ± 39 Ma, respectively. Including systematic error, the weighted mean of these analyses is 1863 ± 31 Ma (2 s.d., MSWD = 0.13), so we take 1900 Ma as the maximum possible depositional age of the Kuncha Formation. If instead we use the ten youngest analyses excluding grain 30, the weighted mean is 1870 ± 15 Ma (2 s.d., MSWD = 0.075), which would indicate a maximum depositional age of 1890 Ma. We prefer 1900 Ma as the maximum depositional age because this is the more conservative interpretation. The ages of some of our young grains are similar to the c. 1867 Ma age of the youngest detrital zircon found by Parrish and Hodges (1996) in the Kuncha Formation exposed in the Langtang region of east-central Nepal.

Zircons from the type lower Fagfog Formation quartzite (sample number 406102) provided 124 usable ages, which were acquired along with 30 standard analyses. For the standards, one standard deviation of the $^{206}Pb^*/^{207}Pb^*$ and $^{206}Pb^*/^{238}U$ ratio was 0.49% and 1.9%, respectively. The dominant spike in this sample's ages is at c. 1800 Ma, and there is also a subordinate peak on its shoulder at c. 1890 Ma (Fig. 8). There are minor peaks older than c. 1890 Ma, the largest of which is at c. 2530 Ma. Grains 8, 92, and 91 gave ages of 1735 ± 19, 1748 ± 20, and 1751 ± 27 Ma, respectively. The weighted mean of these data is 1743 ± 26 Ma including systematic error (2 s.d., MSWD = 0.14), so we interpret 1770 Ma as the maximum possible depositional age for the lower Fagfog Formation. If instead we use the seven youngest analyses, the weighted mean is 1752 ± 18 Ma (2 s.d., MSWD = 0.2), from which we also interpret a maximum depositional age of 1770 Ma.

Type upper Fagfog Formation quartzite zircons (sample 506079) furnished 182 interpretable ages. 33 standard analyses yielded standard deviations of 0.65% and 1.0% for the $^{206}Pb^*/^{207}Pb^*$ and $^{206}Pb^*/^{238}U$ ratios. The largest age peak is at c. 1910 Ma; this peak has an important broadening of the shoulder at c. 1820 Ma, which is near the crystallization age of meta-granites that intrude basal Lesser Himalayan rocks in Nepal (Fig. 8; Kohn et al., 2010). There are additional small peaks older than 1910 Ma, including a prominent broad peak at c. 2570 Ma. Grains 197, 13, and 57 provided ages of 1777 ± 18, 1791 ± 18, and 1795 ± 18 Ma, respectively. Including systematic error, the weighted mean of these ages is 1787 ± 23 Ma (2 s.d., MSWD = 0.22), so we use 1810 Ma as the maximum possible depositional age of the upper Fagfog Formation. This interpretation does not change if grain 102 (1799 ± 18 Ma) is included in the calculation of the weighted mean.

Sample 406089, the southern unknown quartzite in the Modi Khola valley, provided 182 usable ages, which were bracketed by analysis of 49 standards. For the standards, one standard deviation of the $^{206}Pb^*/^{207}Pb^*$ and $^{206}Pb^*/^{238}U$ ratio was 0.55% and 2.0%, respectively. The most prominent spike in this sample's ages lies at c. 1890 Ma (Fig. 8). There are additional small peaks older than 1890 Ma, the largest of which is the broad peak at c. 2540 Ma. This sample has one grain younger than 1760 Ma and only three grains younger than 1800 Ma. Grains 160, 128, and 147 gave ages of 1758 ± 58, 1781 ± 34, and 1793 ± 20 Ma, respectively. Including systematic error, the weighted mean of these ages is 1787 ± 35 Ma (2 s.d., MSWD = 0.17), so we take 1830 Ma as the maximum possible depositional age for this sample. If we use the ten youngest analyses, the weighted mean is 1801 ± 17 Ma (2 s.d., MSWD = 0.15), from which we would interpret a maximum depositional age of 1820 Ma. We use 1830 Ma because this is the more conservative interpretation.

Sample 406020, the northern quartzite of unknown stratigraphic affinity in the Modi Khola valley, yielded 162 interpretable ages. 52 standard analyses gave standard deviations of 0.59% and 1.6% for the $^{206}Pb^*/^{207}Pb^*$ and $^{206}Pb^*/^{238}U$ ratios, respectively. The largest age peak from this sample is at c. 1890 Ma, and there is a broadening of its shoulder at c. 1800 Ma (Fig. 8). There are smaller peaks older than 1890 Ma, and a large, broad peak at c. 2530 Ma. There are no analyses younger than 1770 Ma and only four analyses younger than 1800 Ma. Grains RE-114, RE-64, and RE-23 yielded ages of 1770 ± 34, 1778 ± 28, and 1781 ± 47 Ma, respectively. The weighted mean of these data is 1776 ± 40 Ma including systematic error (2 s.d., MSWD = 0.019), so we interpret 1820 Ma as the maximum possible depositional age for this sample. Using the seven youngest grains in the calculation of the weighted mean does not change our maximum depositional age interpretation.

Zircons from sample KG-1, the unknown quartzite from the Kali Gandaki valley north of the town of Kushma, furnished 92 usable ages. 21 standard analyses yielded standard deviations of 1.2% and 2.1% for the $^{206}Pb^*/^{207}Pb^*$ and $^{206}Pb^*/^{238}U$ ratios, respectively. The dominant spike in this sample's ages is at c. 1790 Ma, and there is a broadening of its shoulder at c. 1870 Ma (Fig. 8). There are additional small peaks older than 1800 Ma, a very broad peak at c. 2570 Ma and a prominent peak at c. 3050 Ma. Grains 38, 90, and 94 provided ages of 1750 ± 34, 1763 ± 18, and 1765 ± 30 Ma, respectively. Including systematic error, the weighted mean of these ages is 1760 ± 33 Ma (2 s.d., MSWD = 0.061), so we take 1800 Ma as the maximum possible depositional age for this sample. For the ten youngest grains, the weighted mean is 1769 ± 17 Ma (2 s.d., MSWD = 0.070), which

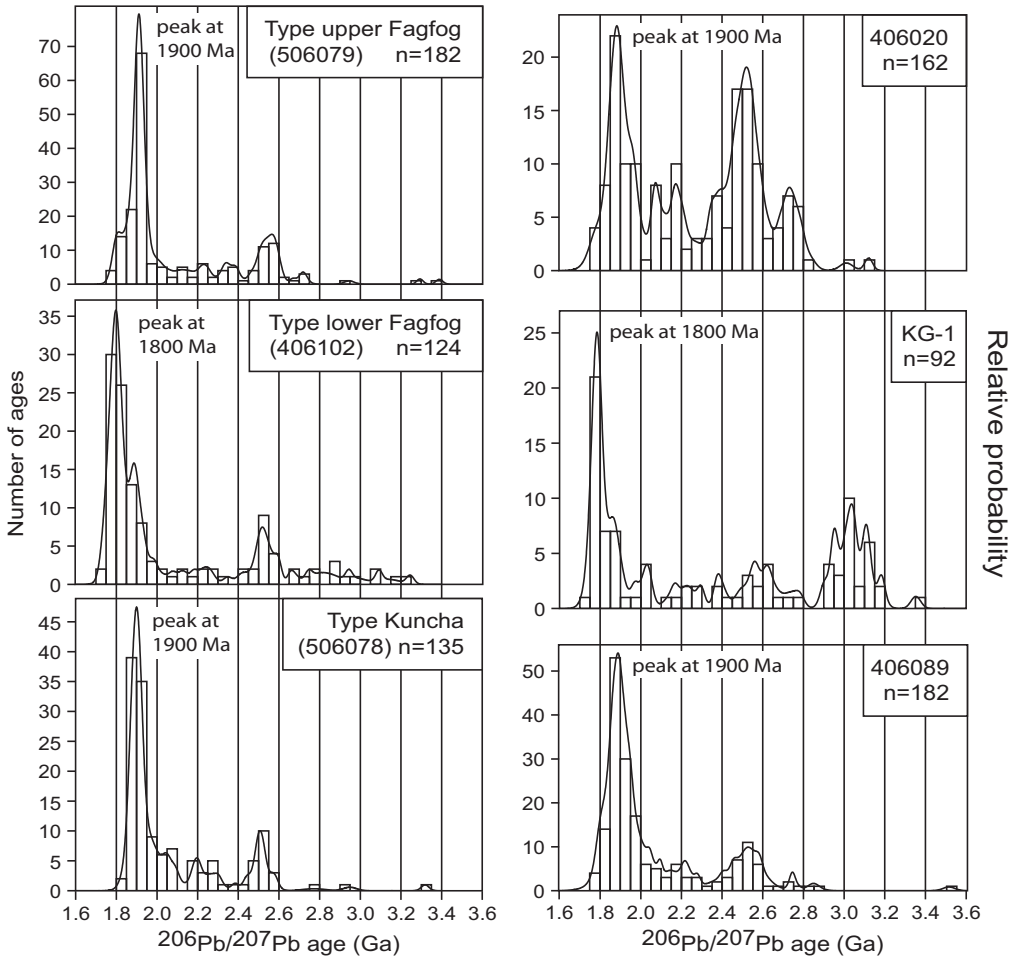

Fig. 8. Relative probability plots (solid lines) and histograms (rectangles) for detrital zircon $^{206}Pb/^{207}Pb$ ages from six samples of Lesser Himalayan rocks. Samples 406020 and 406089 both more closely match the upper Fagfog Formation ages than any other known unit, so we interpret these samples to come from exposures of the upper Fagfog. Sample KG-1 more closely matches the lower Fagfog Formation ages than any other unit, so we interpret this sample to come from an outcrop of the lower Fagfog. The horizontal scale is the same for each plot. Histogram rectangles are 50 Ma wide. Relative probability does not have units.

leads to an estimate of 1790 Ma as the maximum depositional age. We prefer 1800 Ma as the maximum depositional age because this is the more conservative interpretation.

4.2. Malekhu Formation carbonate C isotopic analysis

$\delta^{13}C$ and $\delta^{18}O$ values and lithofacies from the measured section through the type Malekhu Formation are shown in Fig. 9. Photomicrographs of thin sections of these lithofacies are shown in Fig. 3. $\delta^{18}O$ values range from −17 to −9‰, with a mean of -12.4 ± 1.5‰ (1 s.d.). There is a shift toward more negative values above 240 m. In contrast, $\delta^{13}C$ values vary remarkably little throughout the entire 298 m of sampled section. The range is −1.7 to +0.2‰, with a mean of −0.9‰ and one standard deviation of only 0.4‰. Almost all these values come from the analysis of limestone samples, but there is no statistical difference between $\delta^{13}C$ values of limestone and dolostone or calcareous shale. Likewise, there is no correlation between $\delta^{13}C$ values and carbonate grain size.

The trends of the C and O isotopic values through our measured section thus differ considerably. Whereas $\delta^{13}C$ values have a range of only 1.9‰ and little consistent trend throughout the section, $\delta^{18}O$ values have a range of 8‰ and clear trends such as a 7.5‰ negative swing between 240 and 280 m overlain by a 6‰ positive shift between 280 and 335 m. The most negative $\delta^{18}O$ value in the measured section comes from a calcareous shale, and the shift toward more negative $\delta^{18}O$ values near the top of the measured section corresponds to an increasing proportion of calcareous shale in the section, yet there is no relation between $\delta^{13}C$ values and lithology. These disparities in the trends of the C and O isotopes through the section suggest that the $\delta^{18}O$ values were influenced by lithology during alteration from their depositional values by diagenesis and/or metamorphism, but the $\delta^{13}C$ values were not similarly modified and so likely record near-depositional values (cf. Kaufman et al., 1991; Corsetti and Kaufman, 2003). Homogenization of $\delta^{13}C$ values during metamorphism seems unlikely given the large swings in $\delta^{18}O$ values throughout the section (cf. Corsetti and Kaufman, 2003). If $\delta^{13}C$ values were homogenized, we would expect concomitant homogenization of $\delta^{18}O$ values.

There are two possible correlations of the $\delta^{13}C$ trend in our measured section with the known trend for the Proterozoic and Phanerozoic (Fig. 7). Our preferred interpretation is that the Malekhu Formation was deposited during some interval between c. 1770 and 1300 Ma, when marine carbonates recorded only deviations from zero of less than 2‰. By 1250 Ma, $\delta^{13}C$ values were about

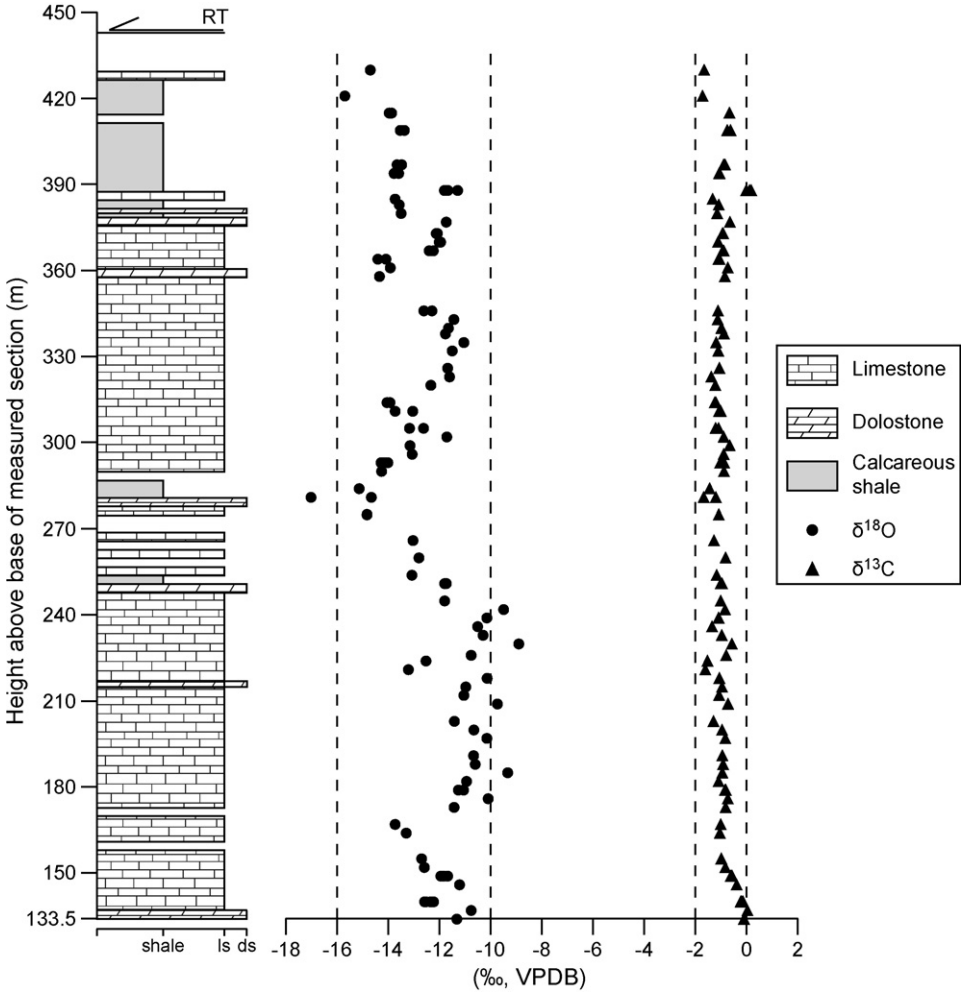

Fig. 9. Lithologies, $\delta^{18}O$ values, and $\delta^{13}C$ values for the measured section through the type exposures of the Malekhu Formation. $\delta^{18}O$ values likely reflect alteration by meteoric or metamorphic aqueous fluids. By comparison with the plot of $\delta^{13}C$ values for marine carbonate throughout the Proterozoic and Phanerozoic (Fig. 7), the limited range of $\delta^{13}C$ values near −1‰ from the measured section suggests deposition of the Malekhu Formation prior to c. 1300 Ma. The section below 133.5 m is covered. Blank areas also represent covered intervals. These rocks have been weakly metamorphosed but are discussed in terms of protolith lithology. Abbreviations: ds – dolostone, ls – limestone, RT – Ramgarh thrust (Pearson and DeCelles, 2005).

+3.5‰, much higher than our highest value of +0.2‰ (Bartley et al., 2001). An alternative interpretation is that the Malekhu Formation was deposited after 1300 Ma during a short stable interval when the carbonate $\delta^{13}C$ value was near −1‰. This scenario requires rapid deposition of the Malekhu so as to not sample any of the more extreme $\delta^{13}C$ values. Although we cannot rule out this possibility, we consider it less likely because we are aware of no c. 1300–500 Ma carbonates that have $\delta^{13}C$ values between −1.7 and +0.2‰ throughout at least 300 m of section (e.g., Kaufman and Knoll, 1995; Kah et al., 1999; Halverson et al., 2005; Maloof et al., 2005; Kaufman et al., 2006, 2007). However, we note that the "Bitter Springs stage" of the Neoproterozoic lower Akademikerbreen Group in northeast Svalbard does have $\delta^{13}C$ values between −1.9 and +0.8‰ throughout a stratigraphic thickness of 250 m (Halverson et al., 2005). It is unlikely that either the Malekhu or the Dhading Formation was deposited in the Phanerozoic because no fossils other than stromatolites and planar-laminated algal structures have been found in any exposure, yet the domal structure of and the fine laminations in the stromatolites are well preserved in both formations (Stocklin, 1980; Upreti et al., 1980; Sakai, 1983, 1985; Upreti, 1996, 1999). Deposition cannot be older than 1770 Ma because the Malekhu sits stratigraphically above the Fagfog Formation, which our detrital zircon U/Pb isotopic ages constrain to have been deposited after 1770 Ma.

5. Implications

5.1. Stratigraphic affinity of the Lesser Himalayan quartzites in the Kali Gandaki and northern Modi Khola valleys

The U/Pb isotopic age spectrum for the detrital zircons from sample 406089 from the southern unknown quartzite in the Modi Khola valley is very similar to the age spectrum from the type upper Fagfog Formation (Fig. 8), so we interpret this quartzite to be within the upper part of the Fagfog Formation (Fig. 5). Key similarities are a prominent age spike near 1900 Ma, a smaller peak near 2550 Ma, and a handful of ages spanning the period 2000–2550 Ma. Further, both samples have only four grains younger than 1800 Ma and only one grain younger than 1780 Ma (Table S1). In contrast, the type lower Fagfog Formation sample yields an age spike at c. 1800 Ma and has 12 grains younger than 1780 Ma and 32 grains younger than 1800 Ma. All type Kuncha Formation zircons are older than c.

1838 Ma, unlike sample 406089, which yielded 15 grains younger than 1838 Ma.

The detrital zircon U/Pb isotopic age spectrum for sample KG-1 is similar, but not identical, to the age spectrum from the type lower Fagfog Formation (Fig. 8). Important similarities are a large age peak near 1800 Ma, a smaller peak near 2550 Ma, and several analyses in the range 1900–2550 Ma. However, sample KG-1 yielded 28 grains between 2900 and 3400 Ma, whereas the type lower Fagfog has only seven zircons in this age range. Despite this difference, the age spectrum for sample KG-1 matches better the spectrum for the type lower Fagfog Formation than the spectra for the type Kuncha and upper Fagfog formations. All type Kuncha zircons are older than c. 1838 Ma, unlike sample KG-1, which yielded 29 grains younger than 1838 Ma. The type upper Fagfog yielded zero grains younger than 1777 Ma and only one zircon younger than 1791 Ma, whereas sample KG-1 has nine grains younger than 1777 Ma and 19 grains younger than 1791 Ma despite only half the total number of analyses. The type upper Fagfog also has its most prominent age spike at c. 1900 Ma, not at c. 1800 Ma as for sample KG-1.

The detrital zircon U/Pb isotopic age spectrum for sample 406020 from the northern unknown quartzite in the Modi Khola valley is not identical to the age spectrum from any of the three type samples (Fig. 8). Sample 406020 yielded six zircons younger than the youngest grain in the type Kuncha Formation, 24 zircons nominally younger than the crystallization age of the granite that intruded the Kuncha in the Langtang region, and two grains nominally younger than the crystallization age of the Ulleri meta-granite, so we rule out the possibility that the northern unknown quartzite belongs to the Kuncha Formation. Although most of the age populations in sample 406020 are also present in the type lower and upper Fagfog samples, the peak near 2550 Ma is much larger in sample 406020. Nevertheless, the U/Pb isotopic ages from sample 406020 appear more like those from the upper part of the Fagfog Formation than from the lower part for two reasons. First, the largest peak in sample 406020 is at c. 1890 Ma with a broadened shoulder at c. 1800 Ma, which is nearly identical to the upper Fagfog type sample but unlike the lower Fagfog type sample, which has its largest peak at c. 1800 Ma and a bump in that shoulder at c. 1900 Ma. Second, sample 406020 has no grains younger than 1770 Ma and only four grains younger than 1800 Ma. This pattern is similar to the upper Fagfog type sample, which has no grains younger than 1778 Ma and only four grains younger than 1800 Ma. In contrast, the lower Fagfog type sample provided seven grains younger than 1770 Ma and 32 grains younger than 1800 Ma. Although the best match of the U/Pb isotopic ages from sample 406020 is with the ages from the type upper Fagfog Formation, the differences in these two age spectra prevent ruling out the possibility that the northern unknown quartzite belongs to the lower part of the Fagfog Formation.

The increased importance of the Archean peak in samples 406020 and KG-1 relative to the other samples may reflect delivery of proportionally more Archean grains to the beds from which we took samples 406020 and KG-1. Alternatively, its increased relative importance may be due in part to higher-temperature metamorphism of the quartzites from which we took these two samples, which are in the hanging wall of the Ramgarh thrust, than of the other sampled rocks, which all lie in its footwall (see Martin et al., 2010a for discussion). Metamorphism may have caused more Pb loss from some of the youngest grains than from the c. 2550 Ma zircons because some of the youngest grains have higher U concentrations (Fig. 10), which increase damage to the crystal from radioactive decay and facilitate diffusion of Pb. These young zircons with high U concentrations and abundant Pb loss then would be preferentially excluded from the age spectrum relative to the older, low-U grains because they would not pass the discordancy filter described in the Methods section.

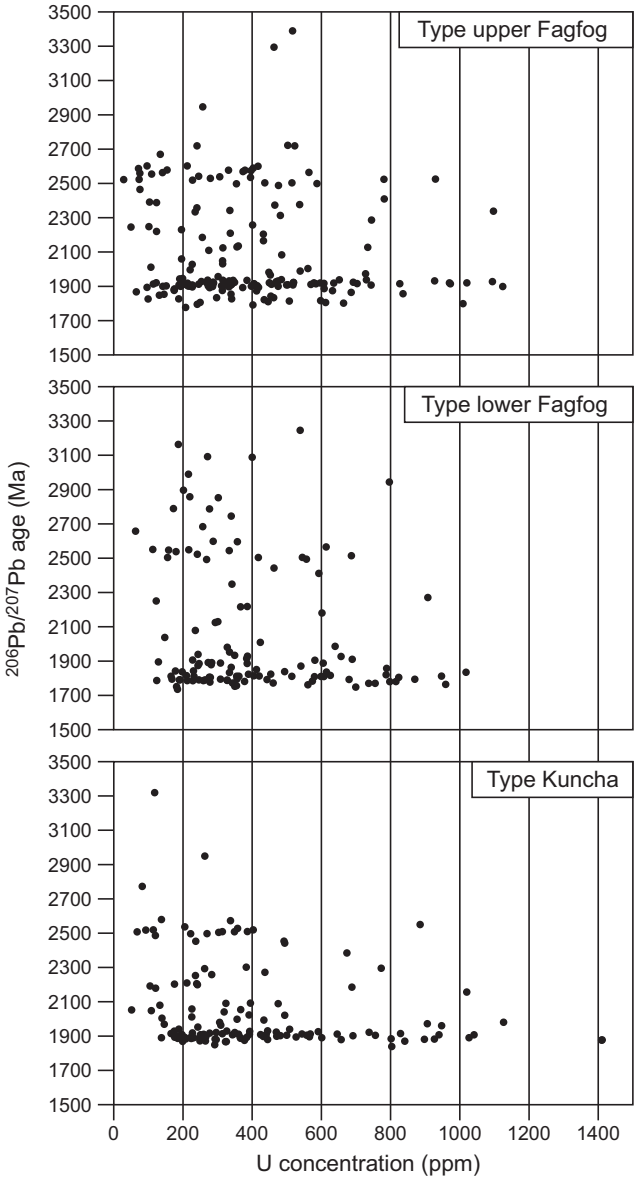

Fig. 10. $^{206}Pb/^{207}Pb$ age versus U concentration for detrital zircons from the type samples of the Kuncha, lower Fagfog, and upper Fagfog formations. In all three samples, the U concentrations of the youngest grains extend to higher values than the c. 2500 Ma crystals. The horizontal scale is the same for all three plots. Error bars are not shown for clarity, but age uncertainties are reported in Table S1 and U concentration errors are less than 20% (Gehrels et al., 2008).

5.2. Stratigraphy at the bottom of the Lesser Himalayan series in central Nepal

5.2.1. Abandonment of the term "Kushma Formation"

Our new detrital zircon U/Pb isotopic ages, combined with field observations, lead us to recommend abandoning the term Kushma Formation in Nepal. At its type locality north of the town of Kushma in central Nepal (near sample 406102), the Kushma Formation passes stratigraphically upward into the Fagfog Formation (near sample 406089) with no obvious hiatus or lithologic difference between the units (Fig. 5). Previous maps show this quartzite-rich succession as a single formation (Tater et al., 1983), and our field observations likewise indicate that it is not possible to discriminate two different formations here – only detrital zircon U/Pb ages allow confident recognition of different units. Instead of two separate formations, we replace the term "Kushma Formation" with

"lower Fagfog Formation," and accordingly name the upper part of the quartzite-rich succession the upper Fagfog Formation.

It is unlikely that the quartzite-rich unit in western Nepal called the Kushma Formation by some workers is correlative with the rocks at the type locality of the Kushma Formation in central Nepal (e.g., Shrestha et al., 1987b,c; DeCelles et al., 1998, 2001; Pearson and DeCelles, 2005; Robinson et al., 2006; Robinson, 2008). DeCelles et al. (2000) showed that, except for one grain that was 32% discordant, U/Pb isotopic ages of detrital zircons from a sample of this basal unit in western Nepal range from 1870 to 1842 Ma, and the youngest cluster of ages is at c. 1860 Ma. In contrast, 45% of the analyzed detrital zircons (56 grains) in our sample from the type locality of the Kushma Formation have U/Pb isotopic ages younger than 1842 Ma, and the youngest cluster of ages is at c. 1750 Ma. Further, in western Nepal the basal quartzite sits stratigraphically below the Ranimata Formation, which contains a c. 1830 Ma meta-granite, indicating that the depositional age of the quartzite is older than c. 1830 Ma (Shrestha et al., 1987b,c; DeCelles et al., 1998, 2000, 2001; Pearson and DeCelles, 2005; Robinson et al., 2006; Robinson, 2008). In contrast, in central Nepal the Kushma Formation was deposited after c. 1770 Ma and rests stratigraphically above the Kuncha Formation, which contains c. 1880 and 1780 Ma meta-granites. Because the basal quartzite-rich unit in western Nepal probably is not correlative with the type Kushma Formation, we recommend that this basal unit be given a new name to distinguish it from the rocks at the type locality of the Kushma Formation.

5.2.2. Order of the Kuncha and Fagfog formations and comparison with previous stratigraphic interpretations

Aside from mostly minor nomenclature differences, our new stratigraphic interpretation is very similar to those by Sakai (1983, 1985) and Dhital et al. (2002), except that we divide their Naudanda Formation into the lower and upper Fagfog Formation. Our stratigraphic column is also similar to those proposed by Stocklin (1980) and Upreti (1996, 1999), except for the division of the Fagfog Formation and the exclusion of the Robang Formation (Fig. 1). This formation was proposed by Stocklin and Bhattarai (1977) and Stocklin (1980) to lie at the stratigraphic top of the Proterozoic part of the Lesser Himalayan series. The Robang Formation has been described only in the Lesser Himalayan rocks directly structurally beneath the Kathmandu nappe; it has never been recognized in the Pokhara-Kali Gandaki region (e.g. Sakai, 1983, 1985; Tater et al., 1983; Dhital et al., 2002). As shown by Pearson and DeCelles (2005), the "Robang Formation" is actually a thrust-repeated slice of the basal units of the Lesser Himalayan series, not an independent formation at the stratigraphic top of the series, so we do not include it in our stratigraphic column.

Unlike these stratigraphic columns, our revised stratigraphic order of the Kuncha and lower Fagfog formations contrasts with the interpretation by Tater et al. (1983), which placed the Kuncha Formation (their Seti Formation) stratigraphically above the lower Fagfog Formation (their Kushma Formation; Fig. 1). Zircon U/Pb isotopic ages indicate that the lowest stratigraphic unit in central Nepal must be the Kuncha Formation, which was deposited after c. 1900 Ma, but before intrusion of both the meta-granite in the Langtang region at 1878 ± 22 Ma and the Ulleri meta-granite at 1780 ± 29 Ma. Thus an interpretation that incorporates the uncertainties on the isotopic ages is that the Kuncha Formation was deposited in some interval between c. 1856 and 1900 Ma. The presence of an 1877 ± 22 Ma (2 s.d., including 1% systematic error) meta-tuff interbedded with the Kuncha Formation strengthens this interpretation (Kohn et al., 2010). The depositional ages of both the lower and upper Fagfog Formation must be younger than the Kuncha because the type lower and upper Fagfog samples both contain multiple zircons younger than the crystallization age of the meta-granite in the Langtang region, outside uncertainty. Further, the type lower Fagfog sample contains multiple zircons that may be younger than the crystallization age of the Ulleri meta-granite, although uncertainties are large enough that the ages overlap within error. The interpretation placing the Kuncha stratigraphically below the Fagfog is supported by the observations that (1) the Ulleri and related meta-granites are nowhere observed to intrude the lower or upper Fagfog, and (2) the lower Fagfog passes stratigraphically upward into the upper Fagfog with no discernable unconformity or lithologic difference in the field, and without the presence of intervening Kuncha Formation rocks. Thus the zircon U/Pb isotopic ages indicate the presence of an unconformity between the Kuncha Formation (deposited between 1900 and 1856 Ma) and the Fagfog Formation (deposited after 1770 Ma) that spans at least 86 M.y. The main uncertainty in this interpretation is the depositional age of the portion of the Kuncha that is stratigraphically above the intrusion level of the meta-granites because the depositional age of this part is not constrained by the crystallization age of the meta-granites. Field evidence suggests that many of the meta-granites intruded near the top of the Kuncha, so the stratigraphic thickness of this portion may be small. Finally, the depositional age of the entire Fagfog Formation also must be younger than the Ranimata Formation of western and eastern Nepal because the Ranimata was intruded by granites at c. 1840–1780 Ma (DeCelles et al., 2000; Kohn et al., 2010).

5.2.3. Importance of stratigraphy for structural mapping

The stratigraphic order of the units is of fundamental importance for structural mapping because repetition and omission of stratigraphy is one of the key methods for recognizing thrust and normal faults. In the Modi Khola valley, incorporation of our new detrital zircon U/Pb isotopic ages results in a very different geologic map for the Lesser Himalayan rocks than that published by Martin et al. (2005). One key difference is the location of the thrust associated with the southern exposure of the Fagfog Formation, which we call the Ramgarh thrust but is called by a different name in previous publications (Fig. 5). Because we now recognize that this quartzite is the Fagfog Formation and that the Kuncha Formation sits stratigraphically below the Fagfog, we now locate the thrust to place the older Kuncha on the younger Fagfog Formation rather than incorrectly inferred older quartzite on inferred younger Kuncha rocks. Another important difference is the sense of motion on the fault that bounds the southern margin of the northern exposure of the Fagfog Formation, which we call the Ghandruk fault. Because we now recognize that this quartzite is the upper Fagfog, and further that the Fagfog Formation is depositionally younger than the Kuncha, we now identify this fault as a normal fault that drops the younger quartzite onto the older Kuncha (omitting the lower Fagfog Formation), rather than a thrust placing incorrectly inferred older quartzite on inferred younger Kuncha metasedimentary rocks. The thickness of the Fagfog is less in the outcrop belt directly north of the town of Ghandruk than in apparently unfaulted areas such as between the towns of Kushma and Birethanti, supporting the interpretation that part of the Fagfog Formation is missing in the belt north of Ghandruk. This northern belt of quartzite is contiguous with the quartzite exposed in the Kali Gandaki valley from which we obtained sample KG-1. If our assignations of samples KG-1 and 406020 to the lower and upper Fagfog formations are correct, the Ghandruk fault must lose separation westward between the Modi Khola and Kali Gandaki valleys because the lower Fagfog is omitted in the Modi Khola valley, but not in the Kali Gandaki valley. We favor the presence of a normal fault to explain this omission because in central Nepal we have not identified stratigraphic termination of major units at the scale of the distance between the Kali Gandaki and Modi Khola valleys (20 km), but we cannot rule out an explanation for the absence of the lower Fagfog north of the town of Ghandruk that relies on stratigraphic vari-

ability created at the time of deposition, without the presence of a fault.

5.2.4. Arguments for intrusion of the Ulleri meta-granite into the Kuncha Formation

Because our analysis of the relative depositional ages of the Kuncha and Fagfog formations depends in part on the interpretation that the Ulleri meta-granite intruded the Kuncha Formation, it is important to present here the arguments that support this interpretation in central Nepal. This discussion is particularly timely because Celerier et al. (2009) suggest that the Ulleri meta-granite in central Nepal and similar intrusive rocks in northwest India might have been the depositional substrate for the lowermost Lesser Himalayan rocks, largely because the maximum possible depositional ages of lower Lesser Himalayan rocks in northwest India appear to be younger than the crystallization ages of the granites (see also Richards et al., 2005; Chambers et al., 2008). This interpretation seems incorrect for the type Ulleri in central Nepal for seven reasons. (1) The maximum possible depositional age of the Kuncha Formation, c. 1900 Ma, is older than the crystallization age of the Ulleri meta-granite, 1780 ± 29 Ma, in contrast to the argument presented by Celerier et al. (2) In the Modi Khola valley of the Annapurna Range, the Kuncha Formation clearly outcrops on both sides of the Ulleri meta-granite (Fig. 5). At a larger scale, the meta-granite apparently is not exposed 20 km to the west in the Kali Gandaki valley nor 15 km to the east in the Seti river valley, so the Kuncha Formation encloses the Ulleri meta-granite on all sides in map view (see also Tater et al., 1983; Amatya and Jnawali, 1994; Larson and Godin, 2009). (3) There are satellite exposures of the meta-granite completely surrounded by the Kuncha Formation, not connected to the main Ulleri pluton in map view (e.g. at 28.33301°N, 83.74464°E; see also description of the 40-m thick, lenticular meta-granite body in the Langtang region by Pearson and DeCelles, 2005). At this location west of the Modi Khola, the Ulleri thickness is on the order of 10 m, and the grain size is much smaller than in the nearby main Ulleri pluton – plagioclase feldspar crystals are up to one cm long, rather than up to five cm. Observations (2) and (3) are more consistent with intrusion of the Ulleri into the Kuncha than with deposition of the Kuncha sediments on the Ulleri granite. (4) West of the type locality at the town of Ulleri, 10 km west of the Modi Khola valley, the meta-granite appears to have a chilled margin (at 28.37850°N, 83.71737°E). Here, plagioclase grains 10 m from the contact with the Kuncha Formation are up to five cm long, whereas plagioclase crystals within 1 m of the contact are no more than one cm long. (5) The Ulleri meta-granite commonly is spatially associated with an unnamed meta-diorite that appears to have intruded the Kuncha Formation. This meta-diorite, like the Ulleri meta-granite, clearly is enclosed in the Kuncha in map view. Further, east of the town of Ulleri, there is an increased abundance of quartz veins in the Kuncha near the contact with the meta-diorite, possibly caused by intrusion of the diorite. The crystallization age of the diorite is unknown, but if it is similar to the crystallization age of the Ulleri meta-granite (see Miller et al., 2000), the intrusive nature of the diorite suggests a similar origin for both. (6) No conglomerate or sandstone obviously derived from the Ulleri meta-granite or the meta-diorite were deposited on the intrusive rocks, as is commonly observed where clastic rocks are deposited on intrusive rocks (e.g., Martin et al., 2010b). (7) We found no zircons with U/Pb crystallization ages within 25 M.y. of the crystallization age of the Ulleri meta-granite (c. 1780 Ma) in the type Kuncha Formation sample, but we analyzed 29 and 6 zircons with this age range in the type lower and upper Fagfog Formation samples, respectively (Table S1). It seems unlikely that the Ulleri and related igneous rocks would have contributed abundant zircons to the Fagfog Formation but not to the Kuncha Formation if the Kuncha sediments were deposited on the meta-granite, between the Ulleri meta-granite and the Fagfog strata.

5.3. East-west correlation of Proterozoic Lesser Himalayan rocks

5.3.1. Correlations at the base of the stratigraphic column

Our new data show that the Kuncha Formation is the basal exposed unit of the Lesser Himalayan series in central Nepal and that, in the Modi Khola and Kali Gandaki regions, it is overlain by the lower part of the Fagfog Formation followed by the upper part (Fig. 5). Farther east, between the Annapurna region and the Kathmandu nappe, it appears that the lower part of the Fagfog Formation is not present. Structurally below the northwestern edge of the Kathmandu nappe, the upper Fagfog Formation sits depositionally on the Kuncha Formation, apparently with no intervening lower Fagfog Formation (Pearson and DeCelles, 2005). Thus the lower Fagfog Formation likely pinches out laterally east of the Modi Khola valley and west of the western edge of the Kathmandu nappe. A more specific location for this lateral termination remains unknown.

5.3.2. Correlations between the Malekhu and Krol units

Some previous studies correlate the Malekhu and/or Dhading formations with limestones of the Krol succession, which is present in the Himalaya of northwest India (Hagen, 1969; Fuchs and Frank, 1970; Sharma et al., 1984; Dhital et al., 2002). The Krol rocks were deposited in the terminal Neoproterozoic Era (Ediacaran Period) and display the large amplitude positive and negative excursions in $\delta^{13}C$ values superimposed on a moderately enriched background typical of carbonates of this age (Aharon et al., 1987; Kaufman et al., 2006; Tewari and Sial, 2007). Our new $\delta^{13}C$ measurements for carbonates from the measured section through the type Malekhu Formation demonstrate that this correlation is unlikely because the Malekhu carbonates have $\delta^{13}C$ values near −1‰ and lack the isotopic excursions found in the Krol rocks. Further, the Krol succession does not correlate with any Lesser Himalayan unit in Nepal because no Neoproterozoic Lesser Himalayan rocks have been found there. Instead, the Krol succession apparently ties best to lower Tethyan Himalayan rocks in Nepal, which contain some similar lithologies and probably were deposited beginning in the Neoproterozoic (Hodges et al., 1996; Gehrels et al., 2003).

5.3.3. Correlations between the Malekhu and Buxa units

The Buxa Formation (sometimes called Buxa Group) is exposed in the Ranjit window of Sikkim, India, approximately 400 km east of our study area. The Buxa Formation in Sikkim is lithologically very similar to the Syangja-Malekhu succession in central Nepal: variegated green, pink, and yellowish-white calcareous slate and intercalated clastic and carbonate rocks near the bottom of the Buxa give way to bluish-gray stromatolitic dolostone at the top (Bhattacharyya and Mitra, 2009). Tewari and Sial (2007) found that $\delta^{13}C$ values from a 700-m thick section of Buxa shallow marine stromatolitic dolostone exposed in the Ranjit window range between only −1.4 and +1.0‰. The similarity of these results to our C isotope stratigraphy for the Malekhu Formation supports a correlation between the two units, although this correlation does not necessarily indicate deposition at exactly the same time. The limited range of C isotopes in the Buxa Formation in Sikkim strongly suggests that the Buxa there was deposited prior to c. 1300 Ma because there is no published example of 700 m of c. 1300–500 Ma carbonate with $\delta^{13}C$ values between only −1.4 and +1.0‰ (e.g., Kaufman and Knoll, 1995; Kah et al., 1999; Halverson et al., 2005; Maloof et al., 2005; Kaufman et al., 2006, 2007). Micropaleontological data suggest deposition of Buxa dolostone exposed in the Ranjit window in the Meso- to Neoproterozoic; the older end of this constraint is consistent with deposition before c. 1300 Ma (Tewari, 2004). The

Buxa Formation in Sikkim is unlikely to have been deposited in the Phanerozoic because stromatolites and microfossils are well preserved in the dolostone, but no other macroscopic fossils have been found (Tewari, 2003; Tewari and Sial, 2007). In contrast to some previous interpretations, correlation of the Malekhu Formation and the Buxa Formation in Sikkim with the shallow marine Menga Limestone, Chillipam Dolostone, and Rupa/Dedza Dolostone some 400 km farther east in Arunachal Pradesh seems unlikely because these eastern carbonates yield $\delta^{13}C$ values between +2.8 and +5.8‰; not one $\delta^{13}C$ measurement overlaps with the Buxa Formation in Sikkim or the Malekhu Formation (Tewari, 2003; Tewari and Sial, 2007). Further, Neoproterozoic-lower Cambrian dolostones in eastern Bhutan previously correlated with the Buxa Formation mostly yield $\delta^{13}C$ values between +3 and +6‰ (Long et al., 2011), and thus perhaps also do not correlate with the pre-1300 Ma Buxa Formation in Sikkim or with the Malekhu Formation.

5.3.4. Unconformity between Proterozoic and Upper Paleozoic Lesser Himalayan rocks

Our new constraint on the minimum possible depositional age of the Malekhu Formation documents the presence of a profound unconformity between the pre-1300 Ma Malekhu and the Carboniferous-Permian Sisne formations, confirming the interpretation of Upreti (1996, 1999). This unconformity spans approximately 900–1400 M.y., depending on the actual depositional ages of the top and bottom of the Malekhu and Sisne formations, respectively. The unconformity appears to be present throughout Nepal because no upper Mesoproterozoic, Neoproterozoic, or lower Paleozoic Lesser Himalayan rocks have been found there. It also likely exists in Sikkim, where Permian Gondwanan clastic rocks rest unconformably on probable pre-1300 Ma Buxa Formation stromatolitic dolostone (Bhattacharyya and Mitra, 2009). In contrast, there are reports of Cambrian Lesser Himalayan rocks to the west in India and to the east in Bhutan (Myrow et al., 2003; McQuarrie et al., 2008; Long et al., 2011). The reasons for these apparent depositional disparities remain obscure, but it seems likely that these and other underappreciated stratigraphic, structural, and metamorphic features inherited from the Proterozoic and Paleozoic impacted the tectonic development of the Himalaya during the Cenozoic.

6. Conclusions

Integration of field observations, detrital zircon U/Pb isotopic ages, and carbonate C isotope values leads to the following conclusions for Proterozoic Lesser Himalayan rocks in central Nepal:

(1) Detrital zircon U/Pb isotopic ages constrain the maximum possible depositional ages for the previously defined Kuncha, Kushma, and Fagfog formations at their type localities in central Nepal to 1900, 1770, and 1810 Ma, respectively.
(2) The incongruous prior use of the term Kushma Formation and our recognition that the Fagfog Formation rests depositionally on the Kushma with no obvious lithologic difference or unconformity between the units in the field lead us to recommend abandoning the term Kushma Formation. We replace "Kushma Formation" with "lower Fagfog Formation" and use "upper Fagfog Formation" for the depositionally overlying part of the unit. Because the 1770 Ma constraint on the maximum possible depositional age comes from the lower part of the Fagfog Formation, the entire formation must have been deposited after 1770 Ma.
(3) Granites intruded the Kuncha Formation at 1878 ± 22 and 1780 ± 29 Ma. The former age, combined with the constraints from the Kuncha detrital zircons, constrain Kuncha deposition to the period 1900–1856 Ma, considering uncertainties. Further, the Kuncha formation must lie stratigraphically below both the lower and upper Fagfog Formations. This conclusion overturns the interpretation of Tater et al. (1983), which placed the lower part of the Fagfog Formation (called the Kushma Formation by these authors) below the Kuncha Formation (called the Seti Formation by these authors). Additionally, any other formation that contains c. 1780–1880 meta-granite, such as the Ranimata Formation of eastern and western Nepal, must have a depositional age that is older than both the lower and upper part of the Fagfog Formation as well.
(4) The zircon U/Pb isotopic ages thus suggest an unconformity of minimum duration 86 M.y. between the Kuncha Formation (deposited between 1900 and 1856 Ma) and the Fagfog Formation (deposited after 1770 Ma).
(5) These new controls on stratigraphy at the base of the Lesser Himalayan series improve structural interpretations in central Nepal by easing previously difficult discrimination between isolated exposures of the lower and upper parts of the Fagfog Formation and by permitting improved location of faults based on repetition or omission of the newly revised stratigraphy.
(6) Carbon isotopes of carbonate from the Malekhu Formation suggest deposition prior to c. 1300 Ma. The Malekhu is stratigraphically above the Fagfog Formation, which has a maximum possible depositional age of 1770 Ma, constraining Malekhu Formation deposition to the period 1770–1300 Ma.
(7) The carbon isotope stratigraphy of the Malekhu Formation is dissimilar to that of the Krol succession in northwest India, indicating that these two units probably are not correlative.
(8) The carbon isotope stratigraphy of the Malekhu Formation matches that of the Buxa Formation exposed in the Ranjit window of Sikkim, supporting a correlation between these two units. However, the carbon isotope stratigraphies of both these formations are different than those of carbonates correlated with the Buxa Formation in eastern Bhutan and Arunachal Pradesh, suggesting that these eastern carbonates do not correlate with the Buxa Formation in Sikkim or the Malekhu Formation in central Nepal.
(9) The Malekhu Formation is unconformably overlain by the Carboniferous-Permian Sisne Formation. The unconformity between the two units spans at least 900 M.y. and rules out the presence of any Neoproterozoic or lower Paleozoic strata in the Lesser Himalayan series in central Nepal.

Acknowledgements

Tank Ojha and the staff of Himalayan Experience provided able field assistance. Philip Piccoli facilitated our use of the electron microprobe, and Victor Valencia enabled our use of the LA-ICMPS. Brendan Williams and Craig Hebert assisted with acquisition of carbonate C and O isotopic data. Peter DeCelles, Ofori Pearson, and Bishal Upreti provided numerous helpful comments on an early draft of the manuscript. Reviewers Nadine McQuarrie and Tom Argles gave constructive reviews, and Randy Parrish provided helpful comments and able editorial handling. Funding for the stable isotope laboratory was provided by NSF grant EAR-0844270 and funding for the Arizona LaserChron Center was provided by NSF grant EAR-0732436.

Appendix A. Supplementary data

Supplementary data associated with this article can be found in the online version at doi:10.1016/j.precamres.2010.11.003.

References

Aharon, P., Schidlowski, M., Singh, I.B., 1987. Chronostratigraphic markers in the end-Precambrian carbon isotope record of the Lesser Himalaya. Nature 327, 699–702.

Amatya, K.M., Jnawali, B.M., 1994. Geological Map of Nepal. Department of Mines and Geology, Government of Nepal, scale 1:1,000,000.

Bartley, J.K., Kah, L.C., 2004. Marine carbon reservoir, Corg-Ccarb coupling, and the evolution of the Proterozoic carbon cycle. Geology 32, 129–132, doi:10.1130/G19939.1.

Bartley, J.K., Semikhatov, M.A., Kaufman, A.J., Knoll, A.H., Pope, M.C., Jacobsen, S.B., 2001. Global events across the Mesoproterozoic–Neoproterozoic boundary: C and Sr isotopic evidence from Siberia. Precambrian Research 111, 165–202.

Beyssac, O., Bollinger, L., Avouac, J.-P., Goffe, B., 2004. Thermal metamorphism in the Lesser Himalaya of Nepal determined from Raman spectroscopy of carbonaceous material. Earth and Planetary Science Letters 225, 233–241, doi:10.1016/j.epsl.2004.05.023.

Bhattacharyya, K., Mitra, G., 2009. A new kinematic evolutionary model for the growth of a duplex—an example from the Rangit duplex, Sikkim Himalaya, India. Gondwana Research 16, 697–715, doi:10.1016/j.gr.2009.07.006.

Brookfield, M.E., 1993. The Himalayan passive margin from Precambrian to Cretaceous times. Sedimentary Geology 84, 1–35.

Buick, R., Des Marais, D.J., Knoll, A.H., 1995. Stable isotopic compositions of carbonates from the Mesoproterozoic Bangemall Group, northwestern Australia. Chemical Geology 123, 153–171.

Burdett, J.W., Grotzinger, J.P., Arthur, M.A., 1990. Did major changes in the stable-isotope composition of Proterozoic seawater occur? Geology 18, 227–230, doi:10.1130/0091-7613(1990)018<0227:DMCITS>2.3.CO;2.

Celerier, J., Harrison, T.M., Webb, A.A.G., Yin, A., 2009. The Kumaun and Garwhal Lesser Himalaya, India. Part 1. Structure and stratigraphy. Geological Society of America Bulletin 121, 1262–1280, doi:10.1130/B26344.1.

Chambers, J.A., Argles, T.W., Horstwood, M.S.A., Harris, N.B.W., Parrish, R.R., Ahmad, T., 2008. Tectonic implications of Palaeoproterozoic anatexis and Late Miocene metamorphism in the Lesser Himalayan Sequence, Sutlej Valley, NW India. Journal of the Geological Society of London 165, 725–737, doi:10.1144/0016-76492007/090.

Corfield, R.I., Searle, M.P., 2000. Crustal shortening estimates across the north Indian continental margin, Ladakh, NW India. In: Treloar, P.J., Searle, M.P., Khan, M.A., Jan, M.Q. (Eds.), Tectonics of the Nanga Parbat Syntaxis and the Western Himalaya, 170. Geological Society of London Special Publication, London, pp. 395–410.

Corsetti, F.A., Kaufman, A.J., 2003. Stratigraphic investigations of carbon isotope anomalies and Neoproterozoic ice ages in Death Valley, California. Geological Society of America Bulletin 115, 916–932.

DeCelles, P.G., Gehrels, G.E., Najman, Y., Martin, A.J., Carter, A., Garzanti, E., 2004. Detrital geochronology and geochemistry of Cretaceous-Early Miocene strata of Nepal: implications for timing and diachroneity of initial Himalayan orogenesis. Earth and Planetary Science Letters 227, 313–330, doi:10.1016/j.epsl.2004.08.019.

DeCelles, P.G., Gehrels, G.E., Quade, J., La Reau, B., Spurlin, M., 2000. Tectonic implications of U–Pb zircon ages of the Himalayan orogenic belt in Nepal. Science 288 (5465), 497–499.

DeCelles, P.G., Gehrels, G.E., Quade, J., Ojha, T.P., Kapp, P.A., Upreti, B.N., 1998. Neogene foreland basin deposits, erosional unroofing, and the kinematic history of the Himalayan fold-thrust belt, western Nepal. Geological Society of America Bulletin 110 (1), 2–21.

DeCelles, P.G., Robinson, D.M., Quade, J., Ojha, T.P., Garzione, C.N., Copeland, P., Upreti, B.N., 2001. Stratigraphy, structure, and tectonic evolution of the Himalayan fold-thrust belt in western Nepal. Tectonics 20, 487–509.

Dhital, M.R., Thapa, P.B., Ando, H., 2002. Geology of the Inner Lesser Himalaya between Kusma and Syangja in Western Nepal, vol. 9. Bulletin of the Department of Geology, Tribhuvan University, Kathmandu, Nepal, pp. 1–60.

Dickinson, W.R., Gehrels, G.E., 2009. Use of U–Pb ages of detrital zircons to infer maximum depositional ages of strata: a test against a Colorado Plateau Mesozoic database. Earth and Planetary Science Letters 288, 115–125, doi:10.1016/j.epsl.2009.09.013.

Fairchild, I.J., Marshall, J.D., Bertrand-Sarfati, J., 1990. Stratigraphic shifts in carbon isotopes from Proterozoic stromatolitic carbonates (Mauritania): influences of primary mineralogy and diagenesis. American Journal of Science 290-A, 46–79.

Fairchild, I.J., Spiro, B., 1987. Petrological and isotopic implications of some contrasting Late Precambrian carbonates. NE Spitsbergen: Sedimentology 34, 973–989, doi:10.1111/j.1365-3091.1987.tb00587.x.

Fike, D.A., Grotzinger, J.P., Pratt, L.M., Summons, R.E., 2006. Oxidation of the Ediacaran Ocean. Nature 444, 744–747, doi:10.1038/nature05345.

Frank, T.D., Lyons, T.W., Lohmann, K.C., 1997. Isotopic evidence for the paleoenvironmental evolution of the Mesoproterozoic Helena Formation, Belt Supergroup, Montana, USA. Geochimica et Cosmochimica Acta 61, 5023–5041.

Fuchs, G., Frank, W., 1970. The geology of west Nepal between the rivers Kali Gandaki and Thulo Bheri: Jahrbuch der Geologischen Bundesanstalt. Sonderband 18, 103.

Gehrels, G.E., DeCelles, P.G., Martin, A., Ojha, T.P., Pinhassi, G., Upreti, B.N., 2003. Initiation of the Himalayan Orogen as an early Paleozoic thin-skinned thrust belt. GSA Today 13 (9), 4–9.

Gehrels, G.E., Valencia, V.A., Ruiz, J., 2008. Enhanced precision, accuracy, efficiency, and spatial resolution of U–Pb ages by laser ablation-multicollector-inductively coupled plasma-mass spectrometry. Geochemistry Geophysics Geosystems 9, Q03017, doi:10.1029/2007GC001805.

Hagen, T., 1969. Report on the Geological Survey of Nepal, vol. 1. Preliminary Reconnaissance. Zurich, Memoires de la societe Helvetique des sciences naturelles, Zurich, p. 185.

Halverson, G.P., Hoffman, P.F., Schrag, D.P., Maloof, A.C., Rice, A.H.N., 2005. Toward a Neoproterozoic composite carbon-isotope record. Geological Society of America Bulletin 117, 1181–1207, doi:10.1130/B25630.1.

Hodges, K.V., Parrish, R.R., Searle, M.P., 1996. Tectonic evolution of the central Annapurna Range, Nepalese Himalayas. Tectonics 15, 1264–1291.

Jacobsen, S.B., Kaufman, A.J., 1999. The Sr, C and O isotopic evolution of Neoproterozoic seawater. Chemical Geology 161, 37–57.

Kah, L.C., Sherman, A.G., Narbonne, G.M., Knoll, A.H., Kaufman, A.J., 1999. $\delta^{13}C$ stratigraphy of the Proterozoic Bylot Supergroup, Baffin Island, Canada: implications for regional lithostratigraphic correlations. Canadian Journal of Earth Sciences 36, 313–332.

Kaufman, A.J., Hayes, J.M., Knoll, A.H., Germs, G.J.B., 1991. Isotopic compositions of carbonates and organic carbon from upper Proterozoic successions in Namibia: stratigraphic variation and the effects of diagenesis and metamorphism. Precambrian Research 49, 301–327, doi:10.1016/0301-9268(91)90039-D.

Kaufman, A.J., Knoll, A.H., Awramik, S.M., 1992. Biostratigraphic and chemostratigraphic correlation of Neoproterozoic sedimentary successions: Upper Tindir Group, northwestern Canada, as a test case. Geology 20, 181–185, doi:10.1130/0091-7613(1992)020<0181:BACCON>2.3.CO;2.

Kaufman, A.J., Knoll, A.H., 1995. Neoproterozoic variations in the C-isotope composition of seawater: stratigraphic and biogeochemical implications. Precambrian Research 73, 27–49.

Kaufman, A.J., Knoll, A.H., Narbonne, G.M., 1997. Isotopes, ice ages, and terminal Proterozoic earth history:. Proceedings of the National Academy of Sciences of the United States of America 94, 6600–6605.

Kaufman, A.J., Jiang, G., Christie-Blick, N., Banerjee, D.M., Rai, V., 2006. Stable isotope record of the terminal Neoproterozoic Krol platform in the Lesser Himalayas of northern India. Precambrian Research 147, 156–185, doi:10.1016/j.precamres.2006.02.007.

Kaufman, A.J., Corsetti, F.A., Varni, M.A., 2007. The effect of rising atmospheric oxygen on carbon and sulfur isotope anomalies in the Neoproterozoic Johnnie Formation, Death Valley, USA. Chemical Geology 237, 47–63, doi:10.1016/j.chemgeo.2006.06.023.

Kaufman, A.J., Sial, A.N., Frimmel, H.E., Misi, A., 2009. Neoproterozoic to Cambrian palaeoclimatic events in southwestern Gondwana. In: Gaucher, C., Sial, A.N., Halverson, G.P., Frimmel, H.E. (Eds.), Neoproterozoic-Cambrian Tectonics, Global Change and Evolution: A Focus on Southwestern Gondwana: Developments in Precambrian Geology, vol. 16. Elsevier, pp. 369–388, doi:10.1016/S0166-2635(09)01626-0.

Knoll, A.H., Hayes, J.M., Kaufman, A.J., Swett, K., Lambert, I.B., 1986. Secular variation in carbon isotope ratios from Upper Proterozoic successions of Svalbard and East Greenland. Nature 321, 832–838, doi:10.1038/321832a0.

Knoll, A.H., Kaufman, A.J., Semikhatov, M.A., 1995. The carbon-isotopic composition of Proterozoic carbonates: Riphean successions from northwestern Siberia (Anabar massif, Turukhansk uplift). American Journal of Science 295, 823–850.

Kohn, M.J., Paul, S.K., Corrie, S.L., 2010. The lower Lesser Himalayan sequence: a Paleoproterozoic arc on the northern margin of the Indian plate. Geological Society of America Bulletin 122, 323–335, doi:10.1130/B26587.1.

Kohn, M.J., Wieland, M., Parkinson, C.D., Upreti, B.N., 2004. Miocene faulting at plate tectonic velocity in the Himalaya of central Nepal. Earth and Planetary Science Letters 228, 299–310.

Kumar, B., Das Sharma, S., Sreenivas, B., Dayal, A.M., Rao, M.N., Dubey, N., Chawla, B.R., 2002. Carbon, oxygen and strontium isotope geochemistry of Proterozoic carbonate rocks of the Vindhyan Basin, central India. Precambrian Research 2002, 43–63.

Larson, K.P., Godin, L., 2009. Kinematics of the Greater Himalayan sequence, Dhaulagiri Himal: implications for the structural framework of central Nepal. Journal of the Geological Society of London 166, 25–43, doi:10.1144/0016-76492007-180.

Lindsay, J.F., Brasier, M.D., 2000. A carbon isotope reference curve for ca. 1700–1575 Ma, McArthur and Mount Isa Basins, northern Australia. Precambrian Research 99, 271–308.

Long, S., McQuarrie, N., Tobgay, T., Rose, C., Gehrels, G., Grujic, D., 2011. Tectonostratigraphy of the Lesser Himalaya of Bhutan: implications for the along-strike stratigraphic continuity of the northern Indian margin. Geological Society of America Bulletin, doi:10.1130/B30202.1.

Maloof, A.C., Schrag, D.P., Crowley, J.L., Bowring, S.A., 2005. An expanded record of Early Cambrian carbon cycling from the Anti-Atlas margin, Morocco. Canadian Journal of Earth Sciences 42, 2195–2216, doi:10.1139/E05-062.

Martin, A.J., DeCelles, P.G., Gehrels, G.E., Patchett, P.J., Isachsen, C., 2005. Isotopic and structural constraints on the location of the Main Central thrust in the Annapurna Range, central Nepal Himalaya. Geological Society of America Bulletin 117, 926–944, doi:10.1130/B25646.1.

Martin, A.J., Gehrels, G.E., DeCelles, P.G., 2007. The tectonic significance of (U, Th)/Pb ages of monazite inclusions in garnet from the Himalaya of central Nepal. Chemical Geology 244, 1–24, doi:10.1016/j.chemgeo.2007.05.003.

Martin, A.J., Ganguly, J., DeCelles, P.G., 2010a. Metamorphism of Greater and Lesser Himalayan rocks exposed in the Modi Khola valley, central Nepal. Contributions to Mineralogy and Petrology 159, 203–223, doi:10.1007/s00410-009-0424-3.

Martin, A.J., Wyld, S.J., Wright, J.E., Bradford, J.H., 2010b. The Lower Cretaceous King Lear Formation, northwest Nevada: implications for Mesozoic orogenesis in the western U.S., Cordillera. Geological Society of America Bulletin 122, 537–562, doi:10.1130/B26555.1.

McFadden, K.A., Huang, J., Chu, X., Jiang, G., Kaufman, A.J., Zhou, C., Yuan, X., Xiao, S., 2008. Pulsed oxidation and biological evolution in the Ediacaran Doushantuo Formation. Proceedings of the National Academy of Sciences of the United States of America 105, 3197–3202, doi:10.1073/pnas.0708336105.

McQuarrie, N., Robinson, D.M., Long, S., Tobgay, T., Grujic, D., Gehrels, G.E., Ducea, M., 2008. Preliminary stratigraphic and structural architecture of Bhutan: implications for the along strike architecture of the Himalayan system. Earth and Planetary Science Letters 272, 105–117, doi:10.1016/j.epsl.2008.04.030.

Miller, C., Klotzli, U., Frank, W., Thoni, M., Grasemann, B., 2000. Proterozoic crustal evolution in the NW Himalaya (India) as recorded by circa 1.80 Ga mafic and 1.84 Ga granitic magmatism. Precambrian Research 103, 191–206.

Misi, A., Kaufman, A.J., Veizer, J., Powis, K., Azmy, K., Boggiani, P.C., Gaucher, C., Teixeira, J.B.G., Sanches, A.L., Iyer, S.S.S., 2007. Chemostratigraphic correlation of Neoproterozoic successions in South America. Chemical Geology 237, 143–167, doi:10.1016/j.chemgeo.2006.06.019.

Myrow, P.M., Hughes, N.C., Paulsen, T.S., Williams, I.S., Parcha, S.K., Thompson, K.R., Bowring, S.A., Peng, S.C., Ahluwalia, A.D., 2003. Integrated tectonostratigraphic analysis of the Himalaya and implications for its tectonic reconstruction. Earth and Planetary Science Letters 212 (3–4), 433–441.

Parrish, R.R., Hodges, K.V., 1996. Isotopic constraints on the age and provenance of the Lesser and Greater Himalayan sequences, Nepalese Himalaya. Geological Society of America Bulletin 108, 904–911.

Pearson, O.N., 2002, Structural evolution of the central Nepal fold-thrust belt and regional tectonic and structural significance of the Ramgarh thrust [Ph.D. Dissertation]: University of Arizona, 231 p.

Pearson, O.N., DeCelles, P.G., 2005. Structural geology and regional tectonic significance of the Ramgarh thrust, Himalayan fold-thrust belt of Nepal. Tectonics 24, TC4008, doi:10.1029/2003TC001617.

Richards, A., Argles, T., Harris, N.B.W., Parrish, R.R., Ahmad, T., Darbyshire, F., Draganits, E., 2005. Himalayan architecture constrained by isotopic tracers from clastic sediments. Earth and Planetary Science Letters 236, 773–796, doi:10.1016/j.epsl.2005.05.034.

Robinson, D.M., 2008. Forward modeling the kinematic sequence of the central Himalayan thrust belt, western Nepal. Geosphere 4, 785–801, doi:10.1130/GES00163.1.

Robinson, D.M., DeCelles, P.G., Copeland, P., 2006. Tectonic evolution of the Himalayan thrust belt in western Nepal: implications for channel flow models. Geological Society of America Bulletin 118, 865–885, doi:10.1130/B25911.1.

Sakai, H., 1983. Geology of the Tansen Group of the Lesser Himalaya in Nepal: memoirs of the Faculty of Science, Kyushu University, Series D. Geology 25 (1), 27–74.

Sakai, H., 1985. Geology of the Kali Gandaki Supergroup of the Lesser Himalayas in Nepal: memoirs of the Faculty of Science, Kyushu University, Series D. Geology 25 (3), 337–397.

Saxena, M.N., 1971. The crystalline axis of the Himalaya: Indian shield and continental drift. Tectonophysics 12, 443–447.

Searle, M.P., 1986. Structural evolution and sequence of thrusting in the High Himalayan, Tibetan–Tethys and Indus suture zones of Zanskar and Ladakh, Western Himalaya. Journal of Structural Geology 8, 923–936.

Sharma, T., Kansakar, R., Kizaki, K., 1984. Geology and tectonics of the region between Kali Gandaki and Bheri rivers in central west Nepal, 38. Bulletin of the College of Science, University of the Ryukyus, pp. 57–102.

Shrestha, S.B., Shrestha, J.N., Sharma, S.R., 1984. Geological Map of Eastern Nepal. Nepal Department of Mines and Geology, scale 1:250,000.

Shrestha, S.B., Shrestha, J.N., Sharma, S.R., 1987a. Geological Map of Central Nepal. Nepal Department of Mines and Geology, scale 1:250,000.

Shrestha, S.B., Shrestha, J.N., Sharma, S.R., 1987b. Geological Map of Mid Western Nepal. Nepal Department of Mines and Geology, scale 1:250,000.

Shrestha, S.B., Shrestha, J.N., Sharma, S.R., 1987c. Geological Map of Far Western Nepal. Nepal Department of Mines and Geology, scale 1:250,000.

Stocklin, J., 1980. Geology of Nepal and its regional frame. Journal of the Geological Society of London 137, 1–34.

Stocklin, J., Bhattarai, K.D., 1977. Geology of the Kathmandu Area and Central Mahabharat Range, Nepal Himalaya. Nepal Department of Mines and Geology/United Nations Development Program, p. 86.

Tater, J.M., Shrestha, S.B., Shrestha, J.N., Sharma, S.R., 1983. Geological Map of Western Central Nepal. Nepal Department of Mines and Geology, scale 1:250,000.

Tewari, V.C., 2003. Sedimentology, palaeobiology and stable isotope chemostratigraphy of the terminal Neoproterozoic Buxa Dolomite, Arunachal Pradesh, NE Lesser Himalaya. Himalayan Geology 24, 1–18.

Tewari, V.C., 2004. Palaeobiology and biosedimentology of the stromatolitic Buxa Dolomite, Ranjit window, Sikkim, NE Lesser Himalaya India. In: Proceedings of the Seventh Conference on Chemical Evolution and the Origin of Life, Trieste, Italy. Kluwer Academic Publishers, The Netherlands.

Tewari, V.C., Sial, A.N., 2007. Neoproterozoic–Early Cambrian isotopic variation and chemostratigraphy of the Lesser Himalaya, India Eastern Gondwana. Chemical Geology 237, 64–88, doi:10.1016/j.chemgeo.2006.06.015.

Tucker, M.E., 1985. Calcitized aragonite ooids and cements from the Late Precambrian Biri Formation of southern Norway. Sedimentary Geology 43, 67–84, doi:10.1016/0037-0738(85)90055-7.

Upreti, B.N., 1996. Stratigraphy of the western Nepal Lesser Himalaya: a synthesis. Journal of Nepal Geological Society 13, 11–28.

Upreti, B.N., 1999. An overview of the stratigraphy and tectonics of the Nepal Himalaya. Journal of Asian Earth Sciences 17, 577–606.

Upreti, B.N., Le Fort, P., 1999. Lesser Himalayan crystalline nappes of Nepal: problems of their origin. In: Macfarlane, A., Sorkhabi, R.B., Quade, J. (Eds.), Himalaya and Tibet: Mountain Roots to Mountain Tops: Special Paper – Geological Society of America. Geological Society of America (GSA), Boulder, CO, United States, pp. 225–238.

Upreti, B.N., Shringarpure, D.M., Merh, S.S., 1980. Stromatolites From the Kali Gandaki Valley Section, Central West Nepal: Their Age, Correlation and Paleoenvironmental Interpretation: Geological Survey of India, 44. Miscellaneous Publications, pp. 255–266.

Valdiya, K.S., 1995. Proterozoic sedimentation and Pan-African geodynamic development in the Himalaya. Precambrian Research 74, 35–55.

Xiao, S., Knoll, A.H., Kaufman, A.J., Yin, L., Zhang, Y., 1997. Neoproterozoic fossils in Mesoproterozoic rocks? Chemostratigraphic resolution of biostratigraphic conundrum from the North China platform. Precambrian Research 84, 197–220.

Zempolich, W.G., Wilkinson, B.H., Lohmann, K.C., 1988. Diagenesis of late Proterozoic carbonates: the Beck Spring Dolomite of eastern California. Journal of Sedimentary Research 58, 656–672.